siraelectro-optics

Technical Note
on

Radiation Effects Analysis Methods

Prepared for QinetiQ plc and ESA ESTEC, The Netherlands

Sira Reference: 245.TN.2/1

Authorised by:
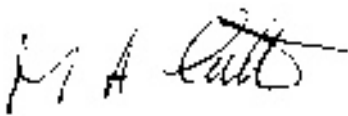
M A Cutter
Technology & Development Manager

Date: April 2002

Abstract

A review of radiation effects analysis methods is given with a view to determining requirements for tools, which are not presently available and priorities for development of new modelling capabilities. The main emphasis is on displacement damage, single event effects and effects on insulators and biological materials. Microdose and dose enhancement effects are also briefly considered.

Executive Summary

This technical note considers radiation effects analysis tools for key areas of importance for future space missions (previously identified in a separate document). Tools in current use will be discussed as well as those, which may need to be developed in future. The note is intended to be read in conjunction with user requirements documents for two suggested new tools (MULASSIS and GEMAT), which have been defined in separate documents by QinetiQ.

Effects, which are linear with total ionizing dose, with no dependence on particle type or devicegeometry, can be predicted knowing the on-orbit dose behind shielding and the experimental device damage coefficients. These are not discussed here as no special analysis tools are needed. This means that the majority of permanent ionization damage effects in integrated circuits are not considered. However micro-dose, dose enhancement, single event effects (SEE) and displacement damage effects, as well as effects in insulators and biological systems are discussed in detail. In many cases it will be seen that the primary need is for improved calculation of the fluences of primary and secondary particles and their associated energy deposition for arbitrary shielding geometries (including graded shielding).

The main conclusions of the study are given below, with cross references to the two suggested new tools (MULASSIS and GEMAT).

Displacement Damage

Displacement damage from secondary particles can be significant and a radiation transport tool is needed to calculate particle flux and deposition behind shielding materials [MULASSIS].

For CCDs (for example) a tool to calculate NIEL deposition in micro-volumes would be useful (e.g. to assess pixel-to-pixel non-uniformity) [GEMAT].

It is usually assumed that displacement damage is proportional to the non-ionizing energy loss produced by a particle. The NIEL hypothesis states that

$$\text{device damage} = K_{damage} \int_{E_2}^{E_1} NIEL(E) \frac{d\phi}{dE} dE$$

Where the damage constant, k_{damage}, has to be determined experimentally. Only one energy (and particle type) is needed if NIEL scaling is valid - but it may be necessary need to establish the validity of NIEL scaling by testing at several energies (and particle types). References to literature on k_{damage} values are given in the text.

Damage can often depend on experimental conditions (e.g. CTE in CCDs), also annealing can be important (e.g. in LEDs and laser diodes) and may have device-to-device variability. Departures from scaling with theoretical NIEL have been demonstrated in some areas (e.g. oxygenated silicon detectors used in high-energy physics, solar cells and LEDs & laser diodes. Hence there is a need for users to be aware of the potential shortcomings of the NIEL approach.

Single Event Upset (SEU) Prediction

In general, adequate tools are available to estimate on-orbit upset rates from cross section data, however there are some particular needs.

It is usually necessary to predict heavy ion and proton upsets separately. Heavy ion induced SEU (produced by direct ionization) is done using cross-section data and the dimensions of the sensitive volume (assuming a rectangular parallelepiped, RPP or IRPP methods). Proton SEU (produced by indirect ionization) is predicted using the Bendel/Petersen (or similar) semi-empirical model (based on nuclear reaction kinetics) and cross section data. If only one set of data is available then methods such as the Petersen figure of Merit (FOM) can be used, but there is a need for more accurate tools to derive one type of SEU rate from another.

The SPENVIS tool (unlike CREME96 or SPACE RADIATION) does not at present allow input of experimental cross sections or Weibull fits (and so does not allow use of the integral RPP method). This is planned as a future upgrade.

The ability to input any user derived particle spectrum would allow better comparison between predicted and observed rates (e.g. for actually observed flare conditions).

Calculation of MBU rates is becoming increasingly important as device geometries shrink and a readily available microsimetry tool [GEMAT] is needed for calculating ionization energy deposition in small volumes (including reaction recoils and products) in order to predict effects for modern devices (e.g. large DRAMs) and to investigate dependence of MBU rate on angle of incidence. Simple cell geometries (without rounded edges) are probably adequate in most cases. This tool would also be useful for prediction of proton single event rates.

There is a need to calculate thermal neutron fluxes in some cases [MULASSIS] (e.g. when there are BPSG overlayers) - and to calculate the effect of the overlayers on secondary production and subsequent charge deposition [GEMAT].

Single event latch up (SEL) and other single event effects can usually be predicted using the SEU methodology discussed above. There is a trend to use 200 MeV proton testing to simulate heavy ion latch-up. It would be desirable for perform more detailed simulation (e.g., using geant4) to validate this approach.

In detector arrays, the calculation of transient events is quite complicated (it involves charge diffusion), but a first cut approach to calculate deposition by secondaries and reaction products in pixel micro-volumes would be useful [GEMAT].

It will need to be considered at some (later) stage how the radiation transport and deposition tools are incorporated into a rate prediction tool.

Effects in Biological Materials

The effects of space radiation on biological materials, and in particular on astronauts, is a subject of increasing importance because of the intended prolonged human activity on the International Space Station and speculated habitation of a lunar colony or a voyage to Mars.

Prediction of effects on astronauts depends on a knowledge, both of the local radiation environment (that is, the environment behind local shielding) and of the biological effects on human beings.

The definition of relevant radiation protection quantities (e.g. dose equivalent, equivalent dose and effective dose) is discussed in the text.

There is little available data for low dose rate irradiations or for protons and high LET (HZE) cosmic rays - so weighting (and quality) factors are not well characterized for the space radiation environment. Also there are concerns for effects in DNA and the central nervous system where cell repair does not occur and biological systems can be susceptible to single particle effects (e.g DNA breaks).

A formalism has been suggested involving risk cross-sections (for each particle) but these are not yet known, and so it is necessary at present to fall back on the conventional quality factor formalism.

Calculation of the hazards for astronauts requires a detailed estimation of the effect of shielding. The contribution to the absorbed dose due to secondary particles produced in the shield can be substantial. For large structures, such as the International Space Station (ISS), the production of secondary neutrons can be particularly important. Hence there is a need for development of improved codes and associated databases for predicting particle transport through graded shielding materials (including simulation of target and ion fragmentation) [MULASSIS].

There is also a need to improve understanding of low dose rate proton and heavy ion effects on biological systems and the estimation of RBE factors and/or risk cross sections.

Effects in Insulators

Insulating materials are used in a large variety of spacecraft applications, for example, adhesives, elastomers, thin films, structural materials (such as carbon fibre reinforced plastic, CFRP), insulators/dielectrics (e.g. for electronics applications) and thermal control coatings.

The damage is normally related in a non-linear way to total ionizing dose. Displacement damage is usually not important due to the disordered nature of the material. It is common for materials to be classified according to 'league tables' giving threshold and failure (or sometimes 25% damage) dose. Data obtained in air is subject to oxidation and hence dose rate effects. If a material is used well within its dose limit then there should be little problem, however if the material exposure is comparable to, or exceeds, the limit dose then further work is recommended (preferably including experimental measurements at representative temperatures and particle type and energy).

It would be useful to have a tool for calculating dose deposition in thin polymer films (including overlayers) [MULASSIS], but otherwise, existing analysis tools (which calculate the total dose and primary particle flux behind shielding) should be adequate in most cases.

Effects in Photonic Devices

The use of photonic devices (such as electro-optic modulators and laser crystals) in space is an emerging area, driven by the large expansion in terrestrial fibre communications applications.

The main effects are due to total ionizing dose and occur at higher levels than generally encountered in the natural space environment. The main need is to characterize new devices for radiation damage and no special requirements for new analysis tools have been identified at this time.

<u>Effects in Optical Materials</u>

Radiation effects in optical materials are primarily caused by ionization damage which induces the formation of colour centres and hence loss in optical transmission. In some cases the ionization damage also produces noticeable changes in refractive index and structural properties (due to compaction).

Optical fibres show complicated non-linear and annealing behaviour but effects not normally very serious for the short lengths used in space (but may be important for special fibres; e.g. polarization-maintaining and Erbium doped fibres).

For optical glasses, dose coefficients are a valid approach within the total dose regime < 1 Mrad and when the relaxation (annealing) effects are not significant (short irradiation times or at low temperatures). If relaxation is important the dose coefficients approach can still be valid and is a useful part of the complete model, which includes annealing. Although annealing effects are pronounced, defect kinetics approaches can be used to extrapolate high dose rate ground test data to the space environment, but this approach is not generally recommended due to the errors involved. Use of long term data (either low dose rate or after long term annealing) should be used whenever possible.

Radiation induced refractive index changes in optical glasses are now well established, but the magnitudes of the changes remain at or below the nominal thresholds for the normal index tolerances in typical optical systems. Cerium doped glasses can be particularly susceptible.

It would appear that, in general, there is not equivalence between dose coefficients for different radiation types (e.g. gamma, electrons, protons). Hence it is important to apply the correct coefficients for each (or an equivalence factor). For some glass types (e.g. with high lead content) there will be a dependence on particle type.

For an optical designer (who does not per se have an expert knowledge of radiation effects physics), the tools required to assess the radiation tolerance of his design are:

- a database of dose coefficients and/or induced absorbtion spectra for all the commonly used and available optical glasses
- an optical and optomechanical design of his system and a radiation sector analysis to give him the absorbed dose levels (dose depth distribution curves) and energy spectra at each component in the system
- a computation tool to convolve the data from the database with his optical design and radiation environment analysis so as to produce a table of induced absorbtion and refractive index change for each component (and the total) system

Existing analysis tools, which calculate the total dose and primary particle flux behind shielding, should be adequate in most cases, however there is a need to establish a database for dose coefficients for commonly used materials.

Single Event Transient Effects in Linear Electronics

Single event effects in linear (bipolar) and mixed signal circuits (operational amplifiers, voltage regulators, comparators, pulse width modulators and ADCs) have emerged as an important threat to spacecraft systems. High-energy particles can deposit charge near internal p-n junctions, which is sufficient to upset the circuit and produce a transient pulse at the output. There is a particular problem if subsequent circuitry can latch the output transient so that it becomes a semi-permanent effect. This tends to occur, for example in voltage comparator circuits that drive digital circuitry.

A range of pulse widths and amplitudes (of either polarity) can be experienced. The parts studied most are amplifiers and voltage comparators (e.g. the LM124 and LM111). It has been found that the transients can depend on bias conditions and circuit values, and will be modified by follow-on circuitry, but transients are difficult to model 'ab initio' since full device details are not usually available from manufacturers and 'reverse engineering' may often be necessary.

For given set of conditions one can measure cross sections experimentally and predict transient rates in the usual way.

It would be desirable to have a device level (equivalent circuit) SPICE model which could simulate the transients and could then be incorporated in a circuit level model. However it is only possible to apply pulses at the input - internal SPICE nodes are not representative - hence hits on internal transistors cannot be simulated.

In this study, B2 PSICE A/D 2000 software was used to provide input transients for OP07, OP37, OP15, LM124, LM218 and CLC426 amplifiers and LM111 and LM218 comparators.

It was found that use of simple 'add-on' SPICE transient pulse generators can give representative transients at device outputs, particularly for operational amplifiers. For voltage comparators the technique does not simulate the dependence of heavy ion transients on differential input voltage which is seen experimentally, but this is to be expected as pulses cannot be applied to the sensitive internal nodes which pertain at high differential input voltages.

The SPICE method can be used as a precursor to device testing and to gauge the effect of external circuitry (e.g. filter capacitors). It has to be emphasised however that simple SPICE modelling cannot fully simulate the complex interactions, which occur in a real device and so can only be used as a rough guide. A recommended technique is simply to use a large amplitude voltage transient (either near-rail-rail, or previously established worst case) at the device output and to perform detailed analysis (or experimental measurements) only if unwanted effects are seen.

An alternative could be to irradiate a device 'in situ' in the circuit, e.g using a 200 MeV proton beam.

Transient Effects in Optocouplers and Fibre-optic Links

In principle, SEU rate prediction for fibre optic data links and optocouplers can be made using the general formalism for SEU prediction. In both cases the most sensitive element for single event upset is the photodetector. This is because the optical signal typically has low power and the electrical signal, which represents a single bit is normally 100-1000 electrons, is easily corrupted by even lightly ionizing particles that strike the detector (which typically has a diameter of several hundred microns).

Care has to be taken to include the angular and energy dependence of proton effects for optocouplers. Modifications to error rate prediction models for optocouplers (e.g. based on CREME96) may be needed in future once a formalism has been accepted.

Dose Enhancement Effects

Dose enhancement occurs in electron and bremsstrahlung environments where high-Z (i.e. high atomic number) materials overlay or are close to the SiO2 layer of a device. The enhancement comes about from departures from radiation equilibrium at an interface with a high-Z coating or from backscatter of Compton electrons (generated by bremsstrahlung) or reflection of electron flux from high-Z layers. High Z materials can be gold coatings, package materials (such as Kovar, gold-plated Kovar or high Z ceramics) or high- Z solder bump-bonds and beam-leads. Enhancements can be an order of magnitude in some cases.

Accurate estimation of dose enhancement effects in high electron environments needs a particle transport code which can calculate electron and bremsstralung fluxes (and the ionising dose produced) for arbitrary shielding geometries which include high Z layers. In this respect a tool, such as MULASSIS may be useful.

Microdose Effects

A single heavy ion can deposit enough dose in the gate oxide above the small sensitive volume of a high-density memory to cause a localized total dose failure (otherwise known as a single Hard error, SHE, or a 'stuck bit'). Stuck bits can also be produced by single event gate rupture. In modern devices the error rate for stuck bits has remained low, probably because of architecture changes and the use of thin gate oxides. However microdose effects still pose a potential threat, particularly for mass memories (DRAMS).

A tool for predicting energy deposition in small volumes could also be used to investigate the likelihood of experiencing single hard errors in MOS circuits [GEMAT].

Effects in Detector Crystals for Space Science Applications

Charge-deposition spectra of ionising radiation in detector materials is a major source of background in astronomy and astrophysics missions ranging from the infrared to the gamma ray. In the latter case the contribution of radioactivity limits sensitivity even outside the regimes of intense particle radiation. Extensive work has been performed on NaI, CsI, bismuth germanate and germanium but further calculations are required for newer materials, such as gadolinium oxyothosilicate, cadmium zinc telluride, barium fluoride. The use of heavy spacecraft and detector systems necessitates the accurate computation of secondary radiation and its spectrum. [MULASSIS]. In modelling activation, there is a need for an optimised technique for producing spallation product and response function libraries.

Use of compound semiconductors for high-energy astrophysics missions has recently been discussed. CdZnTe is a material, which is starting to be considered for space applications. However, the material is prone to radiation-induced carrier (in this case electron) trapping - much more so than hole trapping in germanium (which is commonly used for gamma ray detection). More work on device characterisation is needed, however, before specific requirements on analysis tools can be derived.

List of Abbreviations

ADC	Analogue to Digital Converter
BPSG	Boro Phospho Silicate Glass
CCD	Charge-Coupled Device
CFRP	Carbon Fibre Reinforced Plastic
CNS	Central Nervous System
CTR	Current Transfer Ratio (of an LED)
DRAM	Dynamic Random Access Memory
EDAC	Error Detection And Correction
FOM	Figure of Merit
GCR	Galactic Cosmic Ray
GFRP	Glass Fibre Reinforced Plastic
HRE	Highly Relativistic Event
ISS	International Space Station
LED	light Emitting Diode
LET	Linear Energy Transfer
MBU	Multiple Bit Upset
MCT	Mercury Cadmium Telluride
NIEL	Non Ionizing Energy Loss
RBE	Relative Biological Effectiveness
RPP	Rectangular Parallelepiped
SAA	South Atlantic Anomaly
SDRAM	Synchronous Dynamic Random Access Memory
SEB	Single Event Burnout
SEE	Single Event Effect
SEFI	Single Event Functional Interrupt
SEGR	Single Event Gate Rupture
SET	Single Event Transient
SEU	Single Event Upset
SPE	Solar Particle Event

CONTENTS

1.   INTRODUCTION AND SCOPE

This note is in part fulfilment of milestone 2 of ESA contract 14968/00/NL/EC. It considers radiation effects analysis tools for the key areas identified in work package 1. Tools in current use will be discussed as well as those that may need to be developed. User requirements for selected new tools, which are needed urgently, are defined in separate documents (RD2 and RD3, below). Effects, which are linear with total ionizing dose, with no dependence on particle type or device geometry can be predicted knowing the on-orbit dose behind shielding and the experimental device damage coefficients. These are not discussed here as no special analysis tools are needed. This means that the majority of permanent ionization damage effects in integrated circuits are not considered. However microdose, dose enhancement, single event effects (SEE) and displacement damage effects, as well as effects in insulators and biological systems are discussed in detail. In many cases it will be seen that the primary need is for improved calculation of the fluences of primary and secondary particles and their associated energy deposition for arbitrary shielding geometries (including graded shielding).

1.1   REFERENCE DOCUMENTS

RD1   Report "Space Radiation Effects for Future Technologies and Missions", prepared by QinetiQ Space Department and Sira Electro-optics Ltd, document reference DERA/KIS/SPACE/TR010690/1.0, June 2001.

RD2   User Requirements Document, "Multi-Layered Shielding Simulation Software", document reference QINETIQ/KIS/SPACE/URD011023/0.C\, August 2001 [MULASSIS]

RD3   User Requirements Document, "Geant4 Microdosimetry Analysis Tool", document reference QINETIQ/KIS/SPACE/URD011023/0.C\, August 2001 [GEMAT].

2.   RADIATION EFFECTS ANALYSIS TOOLS

2.1   EFFECTS DUE TO DISPLACEMENT DAMAGE

As discussed RD1, particle radiation causes effects in semiconductor devices by displacement of atoms in the crystalline lattice and the creation of permanent defects within the forbidden band gap. This results in phenomena such as increased leakage currents, charge trapping and reduction in carrier lifetime.

It is usually assumed that for mono-energetic particles the displacement damage effect on a device is proportional to the non-ionizing energy loss (NIEL) of the particle. The constant of proportionality is the damage coefficient K_{damage}, so that

$$\text{device damage} = K_{damage} \times NIEL(E) \times \phi_E \qquad (1)$$

where E is the particle energy and ϕ the particle fluence. The product of NIEL and particle fluence is the 'displacement damage dose' (sometimes called simply the 'dose') - which is a quantity for displacement damage, which is equivalent to the quantity 'total ionizing dose' for ionization damage. Displacement damage dose is usually measured In MeV/g, keV/mg or

similar units. Alternatively it can be related to an equivalent fluence of particles at a particular energy (e.g. 1 MeV neutrons, 1 MeV electrons or 10 MeV protons).

The NIEL hypothesis assumes that K_{damage} is independent of particle type and energy. This follows from the assumption that:

- production of vacancies and interstitials is proportional to the energy of the primary knock on atom (PKA)

- defect production is proportional to vacancy/interstitial production

- device damage is proportional to average defect density

For particles with a range of energies (as would be encountered in space) device damage is predicted using the relation:

$$\text{device damage} = K_{damage}\int_{E_2}^{E_1} NIEL(E)\frac{d\phi}{dE}dE \qquad (2)$$

where the integral is the displacement damage dose for the case where there is a spectrum of particle energies.

In cases where the NIEL hypothesis has been verified, K_{damage} can be experimentally measured at a single particle energy (e.g. for 10 MeV protons), otherwise measurement at several energies will be needed.

Use of equation (2) is straightforward if the differential energy spectrum behind shielding $d\phi(E)/dE$ is known for each particle type. The spectra of primary particles can be calculated using tools such as SPENVIS [1] or ESABASE [2]. However there are no readily available tools within Europe for calculating the spectra of secondary particles. This is discussed further below.

With the assumption that NIEL scaling is valid, equation (2) can be used for displacement damage for any particle type. Though the form of the NIEL curve will be different in each case. The function NIEL(E) will also vary with material type but, in principle, equation (2) can be used for any semiconductor. It has also been used for other materials (such as high temperature superconductors).

For silicon, the NIEL curve for protons has been given in tabulations by Summers et al [3] and Dale et al. [4] and at the website http://sesam.desy.de/~gunnar/Si-dfuncs.html. These functions are plotted in figure 1 (also taken from the same website). In the former tabulations [3,4] the NIEL values are given in keV cm^2/mg and in the latter in MeV mb (and called the displacement damage cross section D). For silicon the conversion between the two units is 100 MeV mb = 2.144 keV cm^2/g. Calculations of proton-on-silicon NIEL for energies in the range 200-1000 MeV have also been carried out by Jun [5] using the MCNPX code, by Alurralde et al. using HETC [6] and by Akkermann et al. [7] using the most recent data bases for differential interaction cross sections (ENDF/B-VI) together with a semi-empirical model to calculate the energy distribution of recoils.. Messenger et al. [8] have reviewed the results and concluded that they are in agreement with their previous data (and figure 1) to within a factor 2, which is considered to be the uncertainty in the calculations.
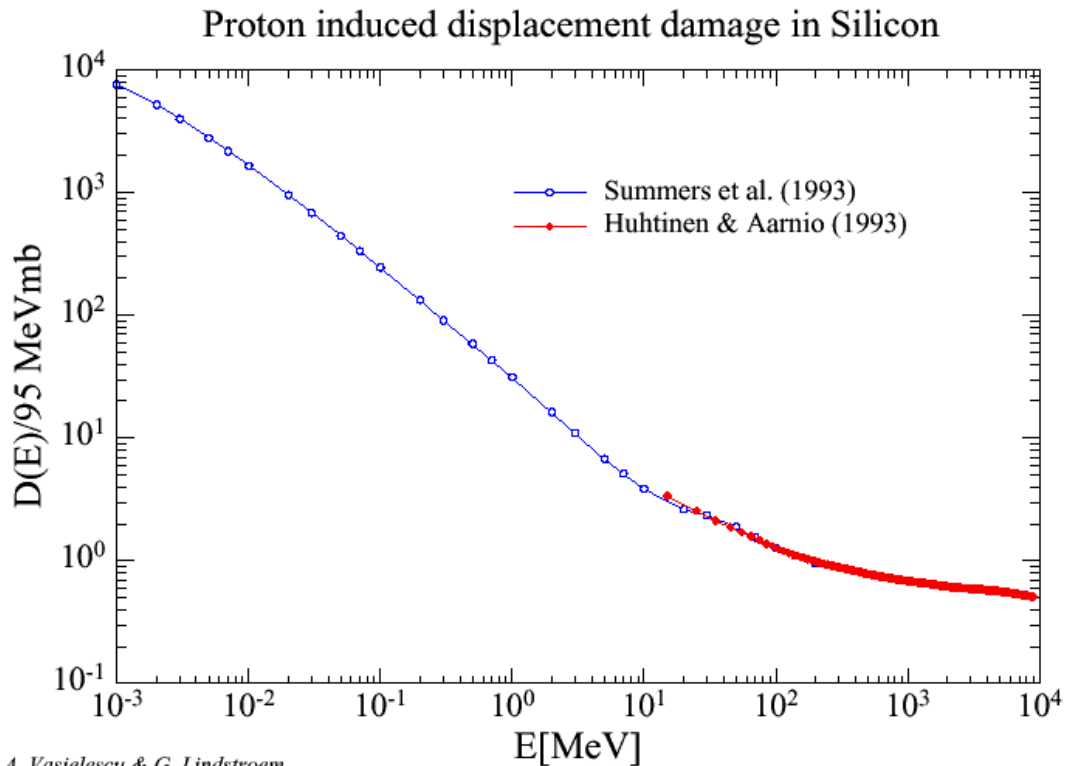
Proton induced displacement damage in Silicon

Figure 1 A. Vasilescu (INPE Bucharest) and G. Lindstroem (University of Hamburg), Displacement damage in silicon, on-line compilation (from http://sesam.desy.de/~gunnar/Si-dfuncs.html)

The above mentioned website also gives details of the NIEL curves for silicon for neutrons, pions and electrons. Curves for other materials can be found in the following references:

GaAs, InP [3]
InGaAs [9]
Ge [10]
SiC [11]

Since the data of Akkerman et al. for Si and GaAs is the most recent, it could be argued that these are the best values to take for these materials. Figure 2 shows a comparison of the NIEL values for protons on silicon with the earlier results of Summers et al [3] (data values from [7] provided directly by the authors [J. Barak, private communication, 2001]). It can be seen that the agreement is good but the new data shows a significant lowering of the NIEL values at high proton energies. For example the ratio of 10 MeV and 60 MeV NIEL differs by a factor 1.5. In contrast data for protons on GaAs show no significant differences between the two data sets [7].

Messenger et al [12] have described an adequate methodology for determining the NIEL current for any material using the SRIM code. However, this does not take into account nuclear inelastic reactions and so will underestimate the damage at high energies where nuclear spallation becomes important.
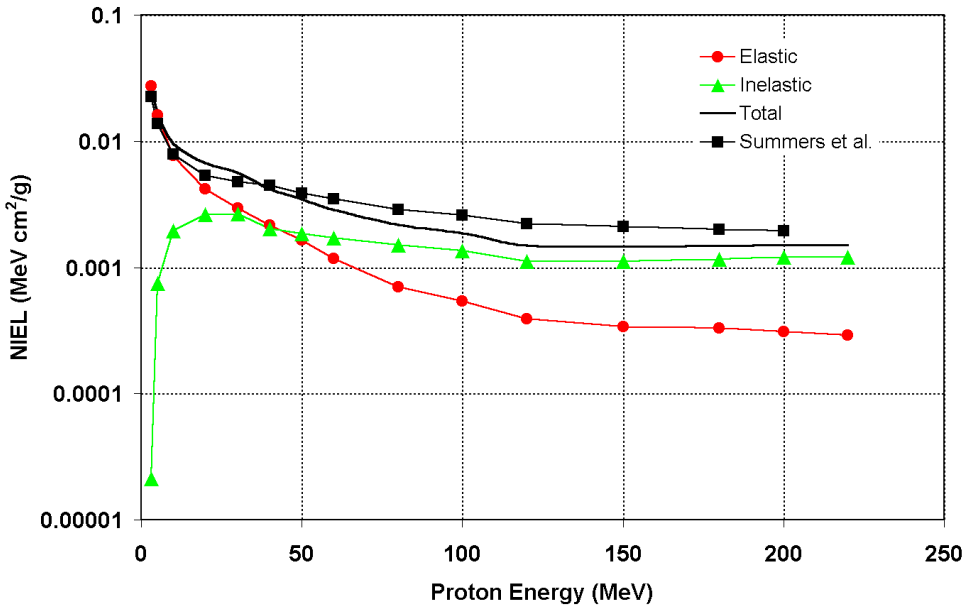
Figure 2 NIEL values for protons on silicon [7] (data provided directly by the authors)

The damage constant K_{damage} will depend on the parameter affected, the particular device type, the material and in some cases the operating conditions. Examples of devices and parameters affected are given in Table 1 below:

Opto-couplers are a case where damage can be a mixture of both displacement damage and ionization effects [13]: displacement damage in the LED (light output affected) and phototransistor (due to lifetime degradation), ionization damage in the phototransistor - due, for example to surface recombination in the lightly doped collector. If displacement damage in the LED dominates then it is the GaAs NIEL, which is important. If the phototransistor response dominates then it is the silicon NIEL that is important.

Table 1 Examples of devices and parameters affected by displacement damage

Device	Parameter Affected
Silicon	
CCDs	average bulk dark current, charge transfer inefficiency
Photodiodes/phototransistors	responsivity (affected by gain and carrier lifetime)
Solar cells	maximum power output, short circuit current, open circuit voltage, fill factor
transistors	gain, h_{fe}
GaAs/InGaAs	
LEDs	light output
Laser diodes	threshold current shift
Opto-couplers	current transfer ratio (CTR)
Solar cells	as for Si solar cells

In incorporating equation (2) into an analysis tool it is simply necessary to have the appropriate damage curve (either the theoretical NIEL or supplied by the user from experimental data) and to interpolate this to the same energy bins as the differential energy spectrum ($d\phi/de$). The damage constant also has to be supplied by the user (as in the SPENVIS [1] tool).

It should be emphasised again that the damage constant may depend on experimental conditions, for example charge transfer in CCDs is notoriously dependent on conditions (see, for example, [14]) and many devices, such as LEDs and laser diodes show annealing effects.

Although the NIEL scaling hypothesis is expected to be useful in most cases in allowing for most of the energy and particle type dependence, there are examples where departures from a strict scaling rule exist. In these cases it may be necessary for the user to use his own experimental damage versus energy curve (to replace the theoretical NIEL curve).

In silicon, departures from NIEL scaling have been observed for oxygenated silicon for high energy physics applications [15] and it is also possible that more detailed investigation of the defects responsible for charge transfer loss in CCDs may reveal departures from the NIEL curve. In CCDs (and other pixelated detectors) there is also a need to consider the differences in energy deposited from one pixel to another since this will affect the variance of the bulk dark current distribution [4]. Departures from radiation equilibrium (where the range of recoil atoms is larger than the pixel dimension) can also be of interest [16]. Typical dimensions of a pixel are 15 µm x 15 µm x 20 µm depth. This leads to a need for a general microdosimetry tool where the user can determine the energy deposited in a specified micro-volume.

For Si, GaAs and InP solar cells the situation is quite complicated. A review has been given by Walters et al. [17]. In n-type devices the damage varies linearly with NIEL for both electrons and protons but with p-type devices the variation is linear for protons but approximately quadratic for electrons. Also, even at a given energy, the damage constants are not the same for protons and electrons. The ratio of the electron and proton damage constants (which Walters et al. term electron to proton [displacement damage] dose ratios R_{ep}) depends on the device parameter concerned.

Hence, for solar cells, the damage has to be worked out separately for electrons and protons. For protons the damage can be worked out as usual using equation (2). For the electrons:

- the damage versus energy relation (assumed to be a power law) has to be measured for at least two electron energies (or for one energy and cobalt60 data) - or else existing data (power law) has to be assumed.
- The electron damage/energy relation then has to be folded with the electron differential energy spectrum to derive an equivalent [displacement damage] dose of 1 MeV electrons D_e (e.g. in MeV/g) or, alternatively, an equivalent fluence of 1 MeV electrons, ϕ_p.
- This is then divided by the R_{ep} value to get the proton displacement damage dose or the equivalent number of 10 MeV protons, ϕ_p. Note that:

.

$$\frac{\phi_e}{\phi_p} = R_{ep} \frac{NIEL_p}{NIEL_e}$$

(3)

Walters et al. give the following values for ϕ_e/ϕ_p, the ratio of the damage equivalent 1MeV electron and 10 MeV proton fluences for maximum power (P_{max}):

Si	~3500
GaAs	~1000
InP	891

Parameters such as P_{max} can be fitted to the empirical relation

$$P_{max} = A - C \log (1 + K_{damage} D_d) \tag{4}$$

Where A, C and K_{damage} are constants for the cell (varying with the device parameter of interest).

The situation for GaAs photonics components (e.g. LEDs, laser diodes and opto-couplers) has been recently discussed in the literature [18]. In some cases the device damage at high energies is less than that predicted from the theoretical NIEL. Until recently it has not been clear if the discrepancies are due to errors in the theoretical NIEL curve or to a dependence of the damage on the type of defects created (which may in turn depend on the particle type and energy). However Messenger et al. [8] have cited new confirmation [7] of the theoretical NIEL curve for GaAs at high energies and have also shown that some previous data follows the Coulomb curve (i.e. the part which does not include non-elastic nuclear interactions). Recent work has also shown that some device types show departures from the total NIEL curve whereas others do not [19]. Different device types may have different damage mechanisms (e.g recombination in the depletion region or diffusion in the bulk) and these may have differing dependencies on the particle type and energy and hence may show experimental data which fall either on the total or the Coulomb NIEL curves (or, in some cases, in between).

For the case of solar cells discussed above, the devices are only lightly shielded by a thin cover glass and most of the damage comes from low energy particles. Hence any departures from the NIEL curve at high energies are not important. For other GaAs devices it is necessary to know the dependence of damage on particle type and energy (for the particular device type) before predictions can be made.

For LEDs the power output (P) is not linear with fluence but varies as [18]

$$\frac{P_0}{P} = (1 + \tau_0 K \phi)^N \tag{5}$$

where P_0 is the initial power output, τ_0 the initial lifetime, K the damage constant and N a constant dependant on the diode design and operating conditions.

Annealing effects are important for LEDs. Johnston and Miyahira [20] give a relation relating power output to the total charge (Q) injected into the device after irradiation:

$$\Gamma(Q) = (\Gamma_0 - \Gamma_f)/(1 + \frac{Q}{Q_{1/2}}) + \Gamma_f \tag{6}$$

where

$$\Gamma = \left(\frac{P_0}{P}\right)^{1/N} - 1 \tag{7}$$

where Γ_0 and Γ_f are the initial and final (after infinite charge) values of the damage and $Q_{1/2}$ is the charge required for half the change to recover.

For laser diodes the change in threshold current is normally considered to be linear with fluence.

From the above it can be seen that damage can usually be related to the non-ionizing energy loss, though in the case of some solar cells this has to be done separately for electrons and protons. However empirical damage constants usually need to be derived by the user from experiments (in some cases at more than one energy and for each particle type).

Although the primary spectrum $d\phi/de$ can be predicted from available environment and radiation transport models, it was pointed out in WP1 that the energy deposited by secondary particles (mainly protons and neutrons) can also be significant – especially for thick shields. Dale et al. [16] have performed calculations using the Langley BRYNTRN code and Jun [5] and Jun and McAlpine [21] using MCNPX; however there is no tool generally available in Europe for predicting secondary particle flux and therefore there is an urgent need for its development. Ideally such a tool would calculate the differential energy spectrum of particles for any shielding composition and geometry, the calculation for spherical shields of a single material would be adequate for many cases.

Conclusion: **There is a need for development of a radiation transport tool to calculate the particle flux and deposition behind shielding materials and also a need for a general <u>microdosimetry</u> tool where the user can determine the energy deposited in a specified micro-volume.**

Users should also be made aware of the shortcomings of the NIEL approach for some cases - and of the dependence of damage constants on device and operating conditions.

2.2 SEU PREDICTION

Methods for predicting single event upset (SEU) rates, have been recently reviewed in detail by Petersen [22]. In this section we give only a brief overview, the reader is referred to [22] and the references therein for further information. Calculations are based on the Linear Energy Transfer (LET) of the particle. The LET, when multiplied by the path length within the active volume (cell) of the device, gives the charge deposited. There is usually a critical charge (Q_c) before effects are noticed - which is proportional to the critical value for the energy deposited in each 'bit' (or sensitive volume) of the device (one electron hole pair is on average created for each 3.6 eV of energy deposited, or put another way $Q_c = E_c/22.5$ pC/MeV, or 1pC/μm of track $= 98$ MeV- cm^2/mg).

Single events are characterised by a plot of the event cross section (the number of events per unit particle fluence) versus the particle LET. However there may be a variation in critical charge for different parts of the circuit, hence the device cross section does not normally have a sharp cut-on value, but rather a smooth curve which has to be determined experimentally. There is, however, a saturation cross-section (defined for high LET) which corresponds to the area of the sensitive volume. There will also be a threshold energy (E_c) where effects first start to be noticed, corresponding to the critical charge of the most sensitive part of the device (or

device cell). This critical LET is then E_c divided by the maximum path length that a particle can traverse in the sensitive volume. Cross section curves are illustrated in figure 3.
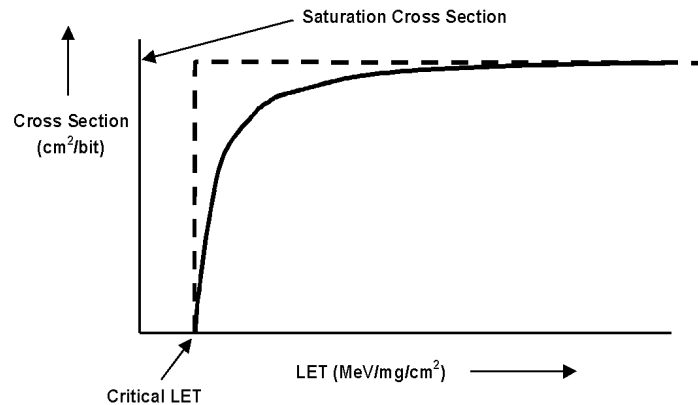

Figure 3 idealised (dashed line) and representative cross section curves

Note that the SEU cross section does not have the same meaning as an interaction cross section in nuclear physics since the path length of the particles has to be included in the calculation of event rates. **It is not correct to simply multiply the cross section curve by the LET spectrum and then integrate.**

For heavy ion cosmic ray irradiation the LET spectrum, f(L)dL, has to be folded with the path length distribution, p(l)dl and the device cross section curve. If we simplify by assuming an idealised curve (dashed line in figure 3) then the event rate is given by

$$U = \frac{S}{4} \int_{Ec/L\max}^{l\max} p(l) \int_{Ec/l}^{L\max} f(L)dLdl$$

(8)

where S is the surface area of the sensitive volume and Lmax the highest LET value.

Usually the sensitive volume is assumed to be a rectangular parallelapiped. Its dimensions are needed in order to calculate the path length distribution (the charge deposited within a track is proportional to the LET multiplied by the path length). These may be known from manufacturers' data but otherwise have to be estimated. Unless charge diffusion is important, the active region area can be taken as the saturation cross section (the cross section at high LET) and **in cases where cross section data or an LET threshold is used** a conservative estimate is obtained by assuming a depth of 1 µm and no funnelling (for small geometry devices this may give a significant overestimate, in which case a 4 µm active region depth can be used) **In cases where a given critical charge is used as an input to derive a prediction then taking zero funnelling does not give a conservative estimate and the actual value of the funnel length (or an over-estimate) has to be used.**

The idealized (rectangular) cross section curve is at present used in the SPENVIS tool [1] but more accurate estimations (that take into account the variations in gain or critical charge within the sensitive volume) can be made using the experimental cross section curve, which is usually fitted to a mathematical function (either a four parameter Weibull or a three parameter log normal distribution). This leads to the integral rectangular parallelapiped (IRPP) method as

described by Petersen [22] and implemented, for example in the SPACERADIATION software suite [23] and CREME96 [24] - and proposed to be implemented in SPENVIS also.

An early paper by Langworthy [25] discussed the effects of the sensitive volume having rounded corners. The effect was to give a gradual slope to the cross section curve rather than a sharp cut-on. However it is now known that a gradual slope is in any case caused by variations in the sensitivity within a cell and so cell rounding was never discussed again.

For proton irradiation only a very few sensitive devices are affected by direct ionization-induced charge but nuclear reactions within shielding material can produce recoil particles with high enough LET to cause effects. Most proton single event calculations use the approach first suggested by Bendel and Petersen [26] who used a semi-empirical approach based on nuclear reaction energetics. There are one- and two-parameter models:

Two parameter proton SEU model:

$$\sigma = \sigma(\infty)[1 - \exp(-0.18Y^{0.5})]^4 \qquad (9)$$

where Y is given by

$$Y = (18/A)^{0.5}(E - A) \qquad (10)$$

where E and A are in MeV and 'A' corresponds to an energy threshold for upset and is fitted to experimental data (at or near 60 MeV). Sometimes $\sigma(\infty)$ is written $(B/A)14$ where B is the Bendel B parameter, in which case the units of σ are 10^{-12} cm^2/bit.

One parameter proton SEU model:

$$\sigma = (24/A)^{14}[1 - \exp(-0.18Y^{0.5})]^4 \qquad (11)$$

Petersen [22] recommends the two parameter approach for modern small geometry devices with saturation cross sections less than 10^{-13} cm^2/bit and that for most parts A can be fixed at 12.5 MeV with only the saturation cross section varying. If there are adequate data then $\sigma(\infty)$ can be obtained from a fit to the Weibull distribution.

In general both proton and heavy ion upset rates need to be calculated but it often occurs (for example in data tabulations for new devices) that only one set is available (usually heavy ion threshold LET and saturation cross section). Petersen [27] and Barak [28] have discussed methods of deriving one set of data from the other. The SPACE RADIATION code [23] offers a module for calculating the proton curve from the heavy ion cross sections and other authors (e.g. [29]) have also discussed methods for generating proton upset data.

The figure of merit (FOM) approach (Petersen [27]) offers a particularly simple method of predicting on-orbit upset rates from either heavy ion or proton data. In his approach the upset rate, R, is given by

$$R = C \times FOM \qquad (12)$$

where C is an orbit specific rate constant and the FOM is derived from heavy ion data using

$$FOM = \frac{\sigma HL}{L_{0.25}^2}\left[\frac{(MeV/mg/cm^2)^2}{cm^2}\right] \tag{13}$$

where σHL is the limiting cross-section per bit and $L_{0.25}$ the LET (in MeV/mg/cm^2) at 25% of the limiting cross section. For proton data we have:

$$FOM = 4.5 \times 10^4 \; \sigma_{PL} \text{ where } \sigma_{PL} \text{ is the proton limiting cross section} \tag{14}$$

To determine $L_{0.25}$, the heavy ion data can be fitted to a Weibull or a lognormal curve. Petersen [22] gives

$$L_{0.25} = L_0 + W + 0.288^{(I/S)} \tag{15}$$

for a Weibull fit with threshold L_0, width W and shape parameter S.

If only a cut off threshold L_0 is known (e.g. from literature data) then the relation:

$$L_{0.25} = 2.77 \; L_0^{0.88} \tag{16}$$

For proton data, σ_{PH} can be estimated from data obtained for energies above 100 MeV.

Petersen gives rate constants, C, for protons and heavy ions as a function of orbit and inclination. The data are presented in graphical form.

Recently, an analytical model for calculating proton-induced SEU cross sections from heavy ion data has been presented by Barak [30], however this approach has not yet been validated.

As noted in the WP1 Report, an important problem which is emerging as device feature sizes shrink is that the probability for multiple bit upsets (MBUs) increases - and also the probability that MBUs will not be corrected by error detection and correction (EDAC) code. There are four recognized mechanisms for MBU:

- Charge diffusion away from an ion track and collection by more than one sensitive node
- Charge collection from a track produced by an ion striking the device at a glancing angle just below the surface such that the track intersects a number of cells in a straight line
- Ion strikes to control circuitry
- Proton- or heavy ion-induced recoils and reaction products intersecting more than one cell (and with either single or multiple secondaries)

Wrobel et al [31] have shown that multi-particle events, where more than one particle (from a reaction outside the sensitive volume) hits the sensitive volume are very rare. Hence the induced reactions, which are important take place in the sensitive volume itself (one particle hits the sensitive volume and produces more than one nucleon). These authors discussed neutron primary irradiations but since the neutron and proton cross sections are the same above 25 MeV [32], the results apply to primary protons also.

Buchner et al [33] have pointed out that most MBUs observed in the proton belt are due to proton-induced recoils, both they and Dyer et al. [34] have discussed situations were simple Hamming EDAC schemes will not correct for MBU and the latter authors have emphasized that the MBU rate is extremely sensitive to the angular distribution of reaction products (which they modelled using HETC). Swift et al [35] have also observed in-flight MBUs in DRAMs.

Recently Wrobel et al. [36] have discussed simulation of MBU rates (using HETC). Their work shows that MBUs can be produced for proton energies greater than 100 MeV. At lower energies the nuclei have too short a range to cause MBU. For multiple secondary MBU events, the deposited energy needs to be less than 0.4 MeV: spallation reactions lead to one recoil (heavy ion) and a shower of light particles with low LET (and hence low energy deposition). For these multiple-secondary neutron or proton MBU events the authors claim that the device has to be sensitive to the light particles (e.g. alphas). Their simulations show that MBU becomes more common as feature sizes decrease. To speed the calculations they used a 128 x 128 structure of spherical sensitive volumes and only ran particular subroutines of the HETC code. For a Geant4-based MBU tool it may be that the size of the array of sensitive volumes will have to be carefully considered if the calculation time is not to be too long.

Hoffman et al. [32] have recently noted a case where anomalous variations in neutron SEU rate where seen in memories, which were coated with a 406µm layer of borophosphosilicate glass (BPSG). This was believed to be due to $^{10}B(n,\alpha)$ reactions. Hence calculation of secondary production in overlayers is likely to be important in some cases.

Finally, it is noted that when comparing observed on-orbit and predicted SEU rates (e.g for technology testbeds such as MPTB and satellites with on-board radiation monitors, e.g. SOHO), it would be useful to be able to use measured on-orbit particle spectra (see for example [37]). This is at present not possible with the SPENVIS tool but is planned for the future.

2.2.1   Single Event Latch-up (SEL)

Testing for single event latch-up is usually performed using heavy ions and cross section data and on-orbit predictions can be performed as for heavy ion SEU rates, discussed above. However O'Niell et al. [38] have shown, using an internuclear cascade - evaporation code, that devices can be screened for latch-up sensitivity using an exposure to 200 MeV protons (using a fluence of 10^{10} p/cm^2 for LEO and 10^{11} p/cm^2 for GEO). This approach has recently been used by Lum et al. [39] and Hiemstra et al. [40]. The advantage is that 200 MeV proton testing can be performed on as-built boards without device de-lidding. It would be desirable to validate the approach using more extensive modelling (e.g. using geant4).

2.2.2   Other Single Event and Transient Effects

Event rates can be calculated using the methods described above for any single event effect or transient events, for which a threshold LET and limiting cross section (or the cross section versus LET curve) are known. This includes single event transient effects in linear devices (discussed in more detail in section 2.7) and single event burn out (SEB) and gate rupture (SEGR).

Transient events are important in all semiconductor detector arrays. The subject has been reviewed in a recent ESA contract report [41]. For CCDs and many IR arrays all particle events are significant, giving event sizes greater than 1000 electrons (as an example, a minimum ionizing particle creates on average ~ 80 electron-hole pairs per µm of track, so for a 15 µm

thickness we have typical events of ~ 1,200 electrons). To predict the total signal in each event just requires the track length and the average number of electrons (W) created for each eV deposited. This is given by [42]

$$W = (14/5)E_g + r, \text{ where } 0.5 < r < 1.0 \text{ eV} \tag{17}$$

Where E_g is the bandgap and r is the energy lost to optical phonons (Raman quanta). Thus the event size can be predicted for any semiconductor material. The table below lists values of W for several materials of interest (for MCT these are calculated, rather than experimental values):

Material	Bandgap (eV)	W (eV)
InSb	0.24	1.1
Ge	0.66	2.9
InGaAs	0.73	3.2
Si	1.12	3.6
GaAs	1.42	4.6
MWIR MCT	0.19	1.3
LWIR MCT	0.12	1.1

Note that the bandgap is normally temperature dependent and so this has to be taken into account for accurate work (e.g. detector calibrations).

To calculate the appearance of the tracks it is necessary to calculate the charge spread by diffusion in the semiconductor [43] and for detailed simulations to consider energy loss straggling [44]. Some events will have a complex nature because of nuclear interactions [45].

Previous studies (e.g. Lomheim et al [46], Dutton et al [47]) have shown good agreement between transient predictions and experimental measurements for CCDs.

There are cases where the transient rate is so high that a background level (with noise) is created. An example is the harsh radiation environment of Jupiter and its moons. In this case it is important to calculate electron transients in detail. A recent study [48] modelled effects using the ACCEPT code from the ITS Monte Carlo electron-phonon transport suite assuming an increased shielding density so that the source disk could be reduced, thus greatly speeding the calculation. Noise from transient events has been discussed recently by Liebe [49] in the context of the Europa Orbiter.

Note that transient effects can also be created by fluorescence and Cerenkov radiation in optical materials (as seen, for example, with Hipparchos).

Although a detailed characterization of the charge appearing in each pixel is complicated, calculation of charge deposited in each pixel micro-volume (without diffusion) will give a first guess at typical event rates and is expected to be worthwhile. Note that for a detector the sensitive volumes would be an array of N x N closely spaced pixel volumes.

Conclusion: **In general, adequate tools are available to estimate on-orbit upset rates from cross-section data, though the ability to input any user derived particle spectrum would allow better comparison between predicted and observed rates (e.g. for actually observed flare conditions). The SPENVIS tool at present accepts only an idealised cross section curve, however CREME96 accepts a table of cross section data as well as Weibull fit parameters. A tool (such as the FOM approach of Petersen) would allow an SEU estimation with limited experimental data (e.g heavy ion but no proton data). Calculation of MBU rates is becoming increasingly important and a readily available tool is needed for calculating ionization energy deposition in small volumes (including secondary particles) in order to predict effects for modern devices (e.g. large DRAMs) and to investigate dependence of MBU rate on angle of incidence. Calculation of secondary-induced charge from reactions in overlayers (e.g. BPSG) is likely be important for environments with significant fluxes of primary or secondary neutrons. Simple cell geometries (without rounded edges) are probably adequate in most cases. Calculation of charge deposited in pixel microvolumes is expected to be useful in estimating transient event rates in detector arrays.**

2.3   EFFECTS IN BIOLOGICAL MATERIALS

2.3.1   Introduction

In this section we discuss the effects of space radiation on biological materials and in particular on astronauts. This is a subject of increasing importance because of the intended prolonged human activity on the International Space Station and speculated habitation of a lunar colony or a voyage to Mars.

Prediction of effects on astronauts depends on knowledge, both of the local radiation environment (that is, the environment behind local shielding) and of the biological effects on human beings. Both are subject to considerable uncertainty and a recommendation of specific radiation tools is beyond the scope of this study. Nevertheless, the discussion may be of interest in developing requirements for further experiments and analysis tools (particularly for radiation transport and fragmentation of heavy ions).

The subject has recently been reviewed in detail by Reitz et al [50] and in two US National Research Council reports, one on 'Radiation Hazards to Crews of Interplanetary Missions' [51] (findings summarized in [52]), and one on 'Radiation and the International Space Station' [53]. A large amount of relevant information is also contained in the proceedings of the NASA 1995 conference on "Shielding Strategies for Human Space Exploration" [54].

Radiobiological effects are classified as

- early (with symptoms appearing over a period anywhere from within minutes of the initial exposure to up to 3-60 days) or

- late (long-term or latent effects)

and also as either

- stochastic (where the probability, but not the severity of an effect increases with exposure and there is no defined threshold)

- non-stochastic (or deterministic) effects where the magnitude or severity of the effect depends on exposure and there is often a threshold dose below which no effect is seen.

Deterministic effects can be early or late, but it can be argued that they are predominantly early effects caused by exposure to a high total dose. Acute effects on the body (somatic, rather than genetic effects) are mass phenomena involving depletion of cells within an organ or tissue. Only after a significant number of cells have been killed is any clinical effect apparent. Hence there is a threshold, usually of order 1Gy (100 rad) or more. The first symptom of radiation 'sickness' is nausea or vomiting, the severity of which increases with dose [51,53]. Acute early effects also include depletion of circulating white blood cells and platelets. As for nausea there is a threshold: in this case typically in the range 1.5-2 Gy [51], although decreases in the white bold cell count can be detected at lower doses.

However the probability is extremely low that the fluxes of radiation inside a spacecraft would be high enough (at least of few Gy) to cause the above effects. Even a prolonged exposure to a solar particle event (SPE) is unlikely to present a major hazard from such 'whole body' effects [51,53]. On the other hand such an exposure could cause skin damage since this 'organ' will receive the highest dose. Temporary sterility is also a possibility for a prolonged SPE exposure. Eye damage, due to formation of cataracts, can also be considered a deterministic effect, though [51] states that the threshold (~1.5 Gy) is more a matter of level of detection and that cataract generation is likely to have a mechanism consistent with stochastic processes.

According to reference [53], highly relativistic (HRE) events (which can give increase in the flux of electrons in the outer belt and are associated with changes in solar wind conditions) can also be severe enough to force an astronaut, performing activities outside the spacecraft, over the short term allowed limit for skin and eye damage (this is for the international space station, which has a high inclination).

In contrast to deterministic effects where large numbers of cells are killed, stochastic effects are often due to single cell effects, for example radiation-induced changes randomly distributed in the DNA of single cells that may lead to cancer or to genetically transmissible effects. Changes to the central nervous system (CNS) may also be important.

Radiobiological effects are predominantly due to ionization processes where bound electrons are ejected from cellular molecules leaving behind chemically active radicals. The result can be recovery, mutation or cell death. If a permanent change occurs then the biological significance will depend on the redundancy of the molecules involved and their function within the cell. However, direct damage to DNA (single or double strand breaks), via protons or heavy ions, is also important. A cell is less likely to recover if several events occur within it. Hence high LET particles (with dense track structures) tend to be more damaging than protons or x-rays.

Repair mechanisms (as for annealing effects in microelectronics) produce a dependence on dose rate and other environmental factors.

2.3.2 Relative Biological Effectiveness (RBE) and the quality factor (Q)

The Relative Biological Effectiveness (RBE) is defined to take the particle dependence into account. It is the ratio of the dose of cobalt60 gamma rays required to produce a specific effect (biological end point) to that required to produce the same effect with the specific particle irradiation.

A large number of RBEs in a wide variety biological systems have been determined and values range between 0.35 and 200 have been found [51]. In terms of defining exposure levels (radiation protection) the quality factor Q is introduced for stochastic effects to account for the different efficiencies of different types of ionizing radiation. The Q factors are established by consensus and reflect a judgement of the importance of the various biological endpoints. and how the empirical RBE values should be weighted.

The RBE factors for protons have been discussed in [53] though it was mentioned that very little experimental information is available. Values in the range 1-3 were reported. In a recent review [55], Yang gives proton RBE values ~1, but data indicates enhanced RBE for small doses of very low energy (<10 MeV) stopping protons and, possibly, for extremely high energy protons (>0.5 GeV).

For heavy ions, the RBE factors can be much larger. Q factors have been defined as a function of LET based on cell killing data and have been recommended by the International Commission on Radiation Protection. $Q_{heavy\ ion}$ (L) is defined as:

$$
\begin{aligned}
Q &= 1.0 & L < 10\ \text{keV}/\mu\text{m} \\
Q &= 0.32L - 2.2 & 10 \leq L \leq 100\ \text{keV}/\mu\text{m} \qquad\qquad (18) \\
Q &= 300/(L)^{1/2} & L > 100\ \text{keV}/\mu\text{m}
\end{aligned}
$$

The reduction in Q(L) for high LET indicates that the cell is not likely to survive and therefore not contribute to carcinogenesis. It has been pointed out however [53] that this function may not always be correct and that the quality factor at high LET can remain high. Yang and Craise (ch. 6 of [54]) indicate that both the energy and the LET have an effect on the biological effectiveness of HZE ions - hence the structure of the track is important.

Since the Q factors vary with particle type they will be different for different orbits. Quality factors for the South Atlantic Anomaly (SAA) vary from 1.6 to 1.9 [53], depending on the shielding and for galactic cosmic rays (GCRs) vary from 2.9 to 3.5 (higher values being associated with higher inclination orbits.

2.3.3 Units for Radiological Protection

The units of dose used for radiological protection have changed over recent years and can be confusing to newcomers to the field. This section gives a brief overview, based on the nomenclature used by Iwai et al. [56]. The terms and definitions are important because they are laid down by international bodies and tend to be embodied in legislation, however they are not specifically focused on space radiation effects (which are mainly caused by low dose rate proton and heavy ion exposure).

We start with the definition of **dose equivalent** (H_R) at a point, for a specific type of radiation, as the product of the absorbed dose (in gray or rad) (D_R) and the quality factor (for that radiation),

Q_R,. Dose equivalent is measured in Sievert (= 100 rem). We can then sum the components to get:

total dose equivalent at a point , $\quad H = \Sigma_R H_R = \Sigma_R Q_R D_R$ $\hspace{3cm}$ (19)

Because the average effect for 'whole body' irradiation is usually required, it is necessary to average the dose over each organ (to give what we term the **averaged organ dose equivalent**, $\overline{H_T}$). This was introduced by the International Commission on Radiation Protection in 1977 [57], which then went on to define the **effective dose equivalent**, H_E, as the weighted sum of dose equivalents of six specified organs (plus a remainder consisting of five organs at most):

$$H_{E,26} = \Sigma_T W_{T,26} \overline{H_T} \hspace{3cm} (20)$$

where $W_{T,26}$ is the tissue weighting factor specified in ICRP26.

Recently, [58] the ICRP published another formulation to take into account the differences in biological effectiveness of the various types of radiation. The **equivalent dose** in tissue ($H_{T,R}$) is again averaged over an organ, but instead of using the quality factor, equivalent dose is defined as the product of the absorbed dose averaged over the organ, multiplied by a weighting factor W_R. This is because of the uncertainties in the radiobiological information for the high-LET part of equation (18), above.

$$H_{T,R} = \Sigma_R W_R D_{T,R} \hspace{3cm} (21)$$

Radiation type		W_R
Photons, all energies		1
Electrons and muons, all energies		1
Neutrons, energy	<10 keV	15
	10 keV – 100 keV	10
	100 keV – 2 MeV	20
	2 MeV – 20 MeV	10
	>20 MeV	5
Protons, other than recoil protons		
	energy >2MeV	5
Alpha particles, fission fragments,		
heavy nuclei		20

In the case of non-uniform distribution of the absorbed dose in the human body the **effective dose** E, is calculated as the weighted sum of equivalent doses ($H_{T,R}$) with weight factors, $W_{T,60}$, recommended by ICRP60 for each organ (and incorporated into the European Union Council Directive 96/29/EURATOM[59]):

$$E = \Sigma_T W_{T,60} H_{T,R} = \Sigma_T W_{T,60} \Sigma_R W_R D_{T,R} \hspace{3cm} (22)$$

Values of $W_{T,60}$ are given below.

Tissue or organ	$W_{T,60}$
Gonads	0.20
Bone Marrow (red)	0.12
Colon	0.12
Lung	0.12
Stomach	0.12
Bladder	0.05
Breast	0.05
Liver	0.05
Oesophagus	0.05
Thyroid	0.05
Skin	0.01
Bone Surface	0.01
Other	0.05

If we have a non-uniform dose, but still use the quality factor (Q) rather than the radiation weighting factor (W_R), then the definition formulated by the International Commission on Radiation Units and Measurements in ICRU51 [60] can be used. This publication defines the **effective dose equivalent**, H_E, as

$$H_E = \sum_T W_{T,60} Q_T D_T = \sum_T W_{T,60} \overline{H}_T \qquad (23)$$

here, D_T and Q_T are the averaged absorbed dose and mean quality factor in a specified tissue (or organ) and Q_T is given by

$$Q_T = \frac{1}{m_T D_T} \int_{m_T} \int_{D_T} Q(L) D(L) dL dm \qquad (24)$$

where m_T is the mass of the tissue or organ T, D(L) is the absorbed dose distribution as a function of LET, L, and Q(L) is the Q-L relationship of ICRP60 (equation 18).

Note that averaging over a whole body so as to calculate effective dose or effective dose equivalent requires the use of anthropomorphic phantom (model) such as ADAM or EVA [61]. Often the irradiation geometry is specified as AP (anterior to posterior) or PA (posterior to anterior).

Radiation monitoring instruments are calibrated in terms of the **ambient dose equivalent**, which is the dose equivalent at a depth of 1 cm in a 30 cm diameter sphere of 4-element ICRU tissue [62]. It is defined so as to be independent of the direction of radiation and also has the advantage of requiring only a simple phantom. Being a dose equivalent (rather than an equivalent dose) the definition uses the quality factor (Q) rather than the weighting factor (W_R).

Another quantity is the **personal dose equivalent**, which is the absorbed dose, weighted by the quality factor, at a depth of 1 cm in a person or calibration phantom. It is the quantity used to calibrate personal dosemeters.

In many cases, where the radiation can be considered to be isotropic, the magnitudes of effective dose and ambient dose equivalent are similar. However Bartlett [63] gives examples (for aircraft altitudes) where effective dose is significantly greater than ambient dose equivalent. Iwai et al. [56] have given conversion coefficients between effective dose and effective dose equivalent and proton and neutron fluence (at various energies).

2.3.4 Further Discussion of Radiobiological Quantities

Some authors have suggested changing the dose quantities by the use of dose modifying factors:

$$N_i = \frac{(DF) \times (PF)}{(DREF)} \qquad (25)$$

where

- DF is a 'dose distribution factor' which accounts for differences in dose depth distribution or partial (or non-uniform) irradiation.

- DREF is a 'dose rate effectiveness factor'. The quality factors are determined mainly from high dose rate terrestrial irradiations and for space applications DREF is usually taken as 2 or 2.5 for space effects [64]

- PF is a 'physiological' factor, which takes into account the biological state of the irradiated tissue, e.g. degree of oxygenation and other stress factors (e.g. zero-gravity effects). The factor will be undetermined in many cases.

Another quantity, which can be defined is the risk. Risk, R, is defined as the likelihood of the occurrence of harmful effects resulting from exposure to radiation and risk factors, k, can be defined such that

$$R = k H \qquad (26)$$

For astronauts, R is usually taken as 3% over an exposure time. This then leads to recommended dose limits [53]:

NCRP recommended dose limits for all organs and ages (in Seiverts)

Limit	Bone Marrow	Eye	Skin
30 days	0.25	1.0	1.5
annual	0.5	2.0	3.0
career	*	2.0	3.0

* Age at exposure	Female	Male
25	0.5	0.8
35	0.9	1.4
35	1.3	2.0
55	1.7	3.0

The 30 day limit is to control early responses which might impact mission safety (lethality, vomiting, nausea), while the annual and career limits are to control cancer risks in later life and depend on the latency period for tumour development and differences in male and female sensitivity. According to [54] these limits are adequate for LEO but are not applicable when significant contributions come from galactic cosmic rays.

As mentioned above, however, estimation of Q factors for high LET (HZE) particles is uncertain. This is a particular problem for long duration exposure. Although damage due to low Z particles may be repaired, this is less likely for higher LET ions (such as Fe). HZE ions can cause damage to a whole column of contiguous highly structured communicating cells such as occur in the central nervous system (CNS) [65]. For instance, damaged neurons may accumulate from heavy ion injury [66]. Also, recent experimental measurements [67] have confirmed that multiple breaks in chromosomes are possible with 1 GeV/micron ions behind polyethylene shields and that these particles are much more effective in producing chromosomal damage than gamma rays.

Note that it has been estimated [68][1] that outside the protection of the Earth's magnetic field each cell nucleus in the body would be hit by a proton once every 3 days, by a helium ion once per month and by higher weight atomic particles (Z>10) once per year, and Curtis et al [66] estimate significant loss rates to brain and retinal cells for a 3 year mission to Mars.

In fact, the methodology of equivalent doses for HZE effects has been questioned [69,70] and a method, which relies on risk cross sections proposed instead.

The risk cross section, σ_i (L) is defined as the probability per unit fluence to directly produce a given effect (e.g. cancer)

$$P = \sum_i r\, \sigma_i (L)\, \phi_i (L)\, dL \qquad (22)$$

In fact the risk cross sections are not known for each particle and [70] relied on the conventional Q factors in its formulation. However the concept may prove useful in future studies.

---

[1] This calculation assumes an area for a cell nucleus of 100 μm^2. The diameter of an average human cell nucleus is ~ 5 to 7 µm so the average nucleus hit rate is possibly somewhat overestimated (by a factor 2-4), but the main argument is unchanged in that most nuclei will be hit during a prolonged space mission.

2.3.5 Effect of Shielding

Calculation of the hazards for astronauts requires a detailed estimation of the effect of shielding. The contribution to the absorbed dose due to secondary particles produced in the shield can be substantial (see for example Cucinotta, [71], Dyer et al. [72]). For large structures, such as the International Space Station (ISS), the production of secondary neutrons can be particularly important [73]. Experimental measurements by Maurer et al. [74] have shown that addition of polyethylene shielding on the ISS can act as a neutron multiplier and actually produce an increase in the dose equivalent.

Calculations of damage due to HZE ions will depend strongly on the fragmentation of these particles as they pass through spacecraft shielding (and through the 20 cm water equivalent of the human body). Use of the HZETRN code has been discussed in [75] but the fragmentation cross sections are uncertain [69,76]. The NUCFRG2 database can be used for heavy ion fragmentation but fragmentation models for light ions requires further work [77]. The effect of target fragmentation on microelectronics SEU calculations (section 2.2) has been discussed by Shinn et al. [78].

Since the nuclear databases are somewhat uncertain at the present time, Wilson et al. [79] have advocated a programme of experimental verification of transmission models. Few measurements have been performed of the biological effectiveness of shielding, but results from Yang et al. [67] illustrate the importance of ion fragmentation and generation of secondaries. They found that chromosomal damage from 250 MeV protons and 1 GeV/u iron nuclei was not diminished by thick (up to 30 cm) slabs of polyethylene shield, even though there was significant attenuation of the primary beam.

The results of shielding calculations also depend on the model used for radiobiological effectiveness. In [69] the conventional Q factor model is compared with shielding calculations for a track structure model. It was found that, as expected, liquid hydrogen was the most efficient shielding material per unit mass and lead the least. In both cases there is a pivotal LET value where the loss of a given ion species due to attenuation is matched by its production, as a secondary, in nuclear events. Above that pivotal LET the flux is increased and below it, decreased. However the shapes of the curves were different for the two damage models. Track structure models have been discussed by Cucinotta et al. [80].

As well as considering secondary production in shielding, Badwhar et al. [81] have pointed out that reentrant electrons can cause significant additional dose. Reentrant electrons are the decay products of nuclear interactions of galactic cosmic rays with the upper atmosophere. These are trapped in the Earth's magnetic field, spiral along field lines, and reenter, in a downward direction in the opposite hemisphere, but at similar latitudes. Although their flux is small their energies extend to several GeV, making them hard to shield against.

In summarising the uncertainties involved in estimating radiobiological effects from HZE ions, Curtis et al [70] suggest a 10-15% uncertainty in the initial charged particle spectra, 50% uncertainty in fragmentation calculations, a factor 2-3 uncertainty in risk coefficients for low-LET radiation and perhaps a factor 2-5 uncertainty in risk cross sections at high LET – thus giving an overall uncertainty of 4-15 in a cosmic ray environment – reference [51] gives uncertainties a factor 2 higher.

2.3.6   Summary

In conclusion, it can be said that there are uncertainties in the prediction of effects on astronauts in the space environment, particularly for prolonged exposure to the cosmic ray environment.   There is a particular need for improved calculation of radiation transport (including production of secondary protons and neutrons and fragmentation of heavy ions) through graded shields and also an experimental measurement of RBE factors as a function of LET (preferably behind various shielding materials).

As a first approximation, risk assessment can make use of terrestrial radiation protection methodologies but the uncertainties involved can be large in some cases.   The present discussion is intended for information purposes and not for guidance on radiation protection (for which official publications should be consulted).

For an approximate estimate of radiation effects it is probably not necessary to use an anthropomorphic phantom. The dose equivalent in a 30 cm slab of tissue is often used (for example in [81]).

Conclusion: **There is a need for development of improved codes and associated databases for predicting particle transport through shielding materials (including simulation of target and ion fragmentation). There is also a need to improve understanding of low dose rate proton and heavy ion effects on biological systems and the estimation of RBE factors and/or risk cross sections.**

2.4   EFFECTS IN INSULATORS

Insulating materials are used in a large variety of spacecraft applications, for example, adhesives, elastomers, thin films, structural materials (such as carbon fibre reinforced plastic, CFRP), insulators/dielectrics (e.g. for electronics applications), thermal control coatings and optical glasses.   The latter we consider in the next section.   Here we look at polymers and CFRP.

In general, effects can be produced at the surface or in the bulk. Surface effects will clearly be most important for thin films but also for unshielded (e.g. structural components) where total ionising dose can be very high (values $\sim 10^9$-10^{10} rad are sometimes quoted for unshielded components for 30 year missions in GEO, however more realistic mission lifetimes are ~ 10 years). In this case much of the damage will be caused by low energy particles, solar X-rays and UV radiation. Bulk damage will be caused by more penetrating radiation. Briskman et al [82] have suggested that the breakpoint for considering only surface damage comes for thicknesses less than $\sim$20 μm and that in this case it is the energy fluence which is important (propagation of defects out of the irradiation layers takes place over distances of 1-10 μm). For thicker materials both surface and bulk effects have to be considered.

Usually, however, it is the <u>total ionizing dose</u> that is taken as the important parameter – but because of the details of the radiation chemistry, which takes place, it can sometimes be that effects depend on the type of particle (i.e. are LET dependent) and on conditions (dose rate, temperature etc.). An important point is that many ground-based measurements are made in air and oxidation plays an important part in the radiolytic reactions (and is responsible for a large proportion of dose rate effects seen in ground-based testing). For measurements to be

truly applicable to space conditions the radiations have to be performed in vacuum or with the test materials surrounded by an inert medium (e.g. liquid nitrogen in the case of cryogenic measurements). In general, materials are tabulated in 'league tables' which usually list the dose for onset of noticeable damage and the maximum useable dose [83].

2.4.1 Polymers

Polymers exhibit a wide range of radiation effects, both temporary and permanent. Temporary effects include radiation-induced outgassing and also charge trapping. Permanent (irreversible) effects are usually more important and result in changes in appearance, chemical or physical state, mechanical, electrical or thermal properties.

All types of radiation (particle or photon) result in excitation and ionization of the polymer chain. After de-excitation and capture of free electrons, chemical radicals (with unpaired electrons) are created and cause reactions, which propagate along the chain or to a side chain. However effects are specific to the chemical structure of the polymer. For example, addition of energy absorbing aromatic rings aids in the distribution of excitation energy in the material so that it does not remain localised in specific sites. Conversely, polymers with highly aliphatic structures (e.g. ethers and alcohols) are the least resistant to radiation [84].

There are two main types of reactions: chain scission and cross linking. The former causes fracture of the molecules and a decrease in Young's modulus, reduced yield stress for plastic flow, increased elongation, decreased hardness and decreased elasticity. Cross linking causes formation of chemical bonds between two adjacent polymer molecules and so an increase in molecular weight. Generally, Young's modulus is increased, elongation is decreased, hardness increased and there is a tendency to embrittlement.

Properties such as Young's modulus, elongation, tensile strength etc. are often non-linear with particle fluence – for example showing threshold effects (c.f. figure 4 [85]). Materials are often tabulated as useful up to a failure dose (see for example [84,86]). Sometimes a threshold for observing effects and a dose for 25% change in properties are listed [87].
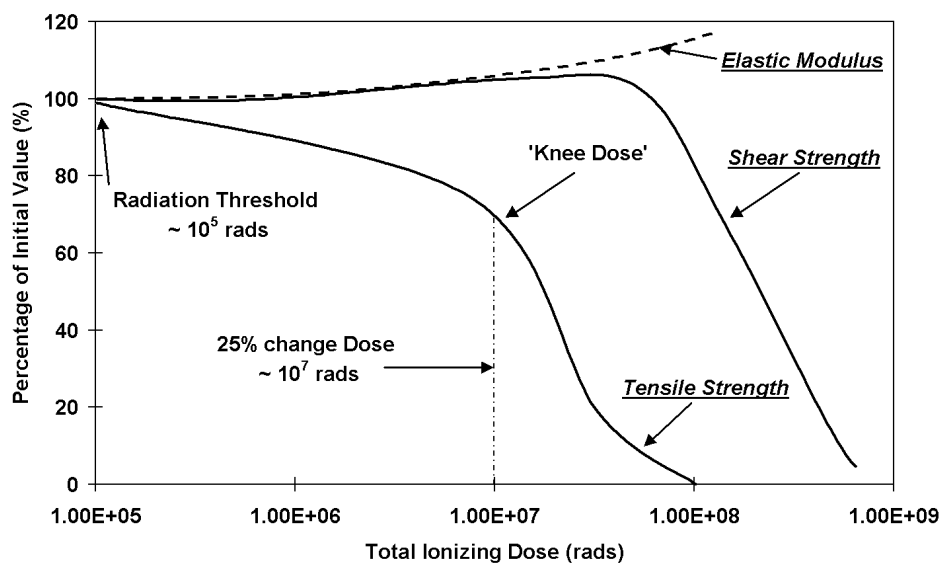

Figure 4 Mechanical properties of typical polymers (e.g. polymethyl methacrylate [87])

It is important to verify that effects are independent of particle type or LET. This has been studied, for example, by Sasuga et al [88]. They found that electron, proton and heavy ion irradiations (in vacuum) gave the same effects (as a function of total ionizing dose) for aliphatic polymers but differences occurred for aromatic polymers (i.e. those containing cyclic structures, such as benzene rings). The trend was for the damage for a given dose to be reduced as LET increases. This is likely to be due to the increased probability of recombination of radicals when the particle track has a high density of excitation.

LET dependent differences in the probability to form cross links were also observed in some polymer materials. If the LET behaviour is not known for a particular material then additional safety margin is needed in calculating acceptable dose levels.

Note that effects differ for irradiation in air (where oxidation reactions are important) compared with irradiations in vacuum or inert gas. Dose rate effects are more important for irradiations in air because of the need for oxygen to diffuse into the material before reactions can occur – but this is not relevant for space applications unless the presence of atomic oxygen is important (as with thin films [86]). Gases evolved during radiolysis can be poisonous or corrosive (for example HCl evolved from PVC [86]).

Tarlet and Ilie [86] mention that in translucent polymers radiation can cause formation of colour centres and hence loss in transmission. Some of these colour centres can be annealed by increase in temperature or photo-bleaching (as in optical glasses, c.f. section 2.5). These authors also note that radioactivity can be induced in some additives (e.g. borinated compounds added as a flame retardant and/or stabiliser) following irradiation by neutrons or high-energy particles.

Frederickson et al. [89] have noted that for good insulators a large electric field can be built up in the material during irradiation. This space-charge field can affect electron trajectories and increase the effective shielding. They found up to a factor 2 enhancement in the shielding effectiveness for slab shileds of polymethylmethacrylate, bombarded with 0.7-2 MeV electrons.

2.4.1.1 Polymer dielectrics

A detailed review of effects in polymer dielectrics has been given by Laghari and Hammond [85]. Electrical parameters which can be affected by high levels (> 10^6 rads) total ionising dose include:

- dielectric strength
- dielectric constant and dielectric loss
- conductivity
- volume and surface resistivity.

As with mechanical properties, these parameters are often non-linear with dose and can show dose rate effects.

Frederickson et al. [90] have recommended that electrically 'leaky' polymers are used as dielectric insulators in space to avoid electrical discharge failures.

2.4.1.2 Elastomers

Elastomers are some of the most sensitive polymer materials. And are used, for example, in seals, gaskets diaphragms etc. Effects are usually tabulated as for polymers in general [91].

2.4.1.3 Effects in polymer matrix composites

Polymer matrix composites (e.g. carbon fibre or glass fibre reinforced plastic – CFRP or GFRP) are good candidates for use as a structural materials in space because of their light weight, high specific strength/stiffness and low coefficient of thermal expansion [92]. For example, CFRP can be useful as a dimensionally stable material for precision antennas and reflectors. For these applications the material potentially suffers both a high total ionising dose and exposure to a range of temperatures.

Radiation effects have been studied by several authors [93,94,95,96]. Amongst the properties that can be affected by total ionizing dose are:

- interlaminar shear strength (ILSS)
- decrease in glass transition temperature (T_g)
- ultimate tensile strength and ultimate strain
- changes in CTE
- susceptibility to microcracking (decrease in the crack initiation energy)

These can be caused, for example, by embrittlement of the matrix due to cross-linking.

As with polymers in general, parameters often show a degradation curve as depicted in figure 2, with degradation starting at a threshold dose. Several authors (e.g. [95], [96], [97]) have noted that the damage threshold can change with conditions (pre-stressing or temperature). Hence comparison between different samples should be made for conditions similar to those pertaining to the flight environment (unless increased safety margins are involved).

Effects will depend primarily on the materials used for the epoxy matrix (and any filters or toughening agents) and will be related to the properties of the matrix itself (rather than the fibres). However, prediction of effects for i materials, based on their chemical structure, does not appear to be feasible at this time.

2.4.1.4 Effects in Thin Polymer Films

Polymer thin films are used as coatings (e.g. for optics [98]) and for proposed applications such as solar sails. As well as polymer degradation as discussed above, properties such as solar absorption can be affected [99]. Because the material exists in a thin layer the main contributors to total dose damage for unshielded samples are low energy electrons and protons. Alstatt and Edwards [100] point out that there is a need for a code for calculation of isotropic proton irradiation of thin materials and also for calculating the secondary neutrons from, for example, aluminium(p,2n) reactions (e.g. in aluminised Teflon foils). These calculations could be produced by the suggested general purpose transport tools discussed above.

Conclusion: **In insulator materials the damage is normally related in a non-linear way to total ionizing dose. Displacement damage is usually not important due to the disordered nature of the material. It is common for materials to be classified according to 'league tables' giving threshold and failure (or sometimes 25% damage) dose. If a material is used well within its dose limit then there should be little problem, however if the material exposure is comparable to, or exceeds, the limit dose then further work is recommended (preferably including experimental measurements at representative temperatures and particle type and energy). Existing analysis tools which calculate the total dose and primary particle flux behind shielding should be adequate in most cases.**

   It would be useful to have a tool for calculating dose deposition in thin polymer films (including overlayers)

2.5   EFFECTS IN PHOTONIC DEVICES

In this section we briefly discuss effects in photonic devices such as electro-optic modulators and laser crystals. This is a rapidly developing field driven by the large expansion in terrestrial fibre communications applications. Effects in polymer, insulator and semiconductor modulators have been discussed by Barnes and Greenwell [101] (see also Barnes et al [102]). The main effects are due to total ionizing dose. They occur at higher levels than generally encountered in the natural space environment. The same applies for most other devices (reference [103] discusses laser crystals). The main need is to be to characterize new devices for radiation damage and no specific requirements for new analysis tools have been identified at this time.

Roth et al. [104] have recently reported on gamma and proton radiation effects in nonlinear crystals (BBO, LBO and KTP) for second harmonic generation (SHG). Only the KTP crystal was significantly affected by levels (~ 100 krad) appropriate to a high dose space environment. Both optical transmission (at wavelengths around480-650 nm) and SHG signal were affected in KTP. Mechanisms were not discussed but it is likely that effects are due to total ionizing dose.

2.6   EFFECTS IN OPTICAL MATERIALS

Radiation effects in optical materials are primarily caused by ionization damage which induces the formation of colour centres and hence loss in optical transmission. In some cases the ionization damage also produces noticeable changes in refractive index and structural properties (due to compaction).

For optical fibres Griscom et al [105] have discussed a power law dependence for transmission loss:

$$L = CD^f \tag{23}$$

where D is the ionizing dose and C and f (<1) are environment constants. They go on to show how annealing effects can be predicted in ground based experiments from knowledge of f and the irradiation time (see also [106,107,108]). At high doses, fibres often show non-linearities and saturation effects. However, the low doses experienced in space, the short lengths used and the annealing (both thermal and photo-bleaching) which takes place all combine to suggest that radiation effects are not a significant issue except for special cases such as Erbium doped

fibre amplifiers ([109] and references therein) and polarization-maintaining fibres [110] where further work is needed.

This is not necessarily the case for optical systems however, where Fruit et al [111] have discussed the use of the dose coefficient approach, where transmission loss and refractive index changes are assumed to be linear with total ionizing dose, at least for doses < 1 Mrad.

Although in many cases the effects will be dependent on total dose, independent of particle type, Marker et al [112] have described cases where there is a dependence on the particle type: where the glass system contains a high amount of lead in non-bonding sites then electron irradiation can lead to reduction to metallic leads and so an increase in discoloration. They also mention that borosilicate glasses can be susceptible to neutron-irradiation due to the high cross section for neutron interaction. Comparisons between proton and cobalt60 irradiations have also been made by Fruit et al. [113], although the results are rather inconclusive at this stage (but it does appear that the dose coefficients depend on radiation type [114]). It appears from recent work [114] that the magnitude of refractive index changes are similar to, or below, typical tolerances for optical systems, but cerium doped glasses can be particularly susceptible.

Structural stability is most important for large optical structures. Radiation induced compaction in Zerodur has been discussed relatively recently by Edwards et al [115]. These authors suggested a power law, as in equation (3), with the parameters C and f being dependent on proton energy. Earlier electron-irradiation results of Higby et al [116] showed a somewhat different power law dependence possibly due to the different type of irradiation.

Changes in density, coupled with a non-unifrom dose distribution can produce distortion of large mirrors. Merzbacher et al. [117] calculated that for 10 years in a 3700 km /30 deg orbit, a displacement of 2500 µm could be produced at the edge of a 4m diameter, 0.5 cm thick zerodur disk (for a silica disk the distortion was negligible). For 10 years in a 1200 km / 98 deg orbit the Zerodur distortion was 205 µm. However use of SiC reinforcement reduced the distortion by an order of magnitude.

In materials, such as Zerodur, that normally have a near-zero coefficient of thermal expansion, radiation-induced defect centres at the interface between glassy and crystalline phases can cause a de-coupling of the thermal expansion of the two phases [118]. Also, the compaction of the high-silica glassy phase and the expansion of the crystalline phase can place additional strain at the interface. The effect is to shift the expansion behaviour to more like that of fused silicas.

Conclusion: **In optical glasses the main effect is radiation-induced absorption due to colour centre formation by total ionizing dose. In some cases, refractive index changes and mechanical compaction can also be important. Annealing effects are pronounced and although defect kinetics approaches can be used to extrapolate high dose rate ground test data to the space environment, this approach is not recommended due to the errors involved. Use of long term data (either low dose rate or after long term annealing) should be used whenever possible. For some glass types (e.g. high lead content) there will be a dependence on particle type. Existing analysis tools, which calculate the total dose and primary particle flux behind shielding should be adequate in most cases, however there is a lack of knowledge of the behaviour (dose coefficients) for many materials.**

2.7 SINGLE EVENT TRANSIENT EFFECTS IN LINEAR ELECTRONICS

Single event effects in linear (bipolar) and mixed signal circuits (operational amplifiers, voltage regulators, comparators, pulse width modulators and ADCs) have emerged as an important threat to spacecraft systems. High-energy particles can deposit charge near internal p-n junctions which is sufficient to upset the circuit and produce a transient pulse at the output. There is a particular problem if subsequent circuitry can latch the output transient so that it becomes a semi-permanent effect. This tends to occur, for example in voltage comparator circuits that drive digital circuitry. The production of transient effects has been discussed by several authors [119,120,121,122,123,124,125,126,127,128,129,130,131,132] and a recent compendium has been presented by Savage et al. [133].

A wide range of pulse widths and amplitudes have been reported and a sensitivity to bias and circuit configuration (e.g. resistor values). Either polarity of pulse can be produced. The most studied parts have been operational amplifiers and voltage comparators, in particular the LM124 amplifier and the LM111 and LM139 comparators. A pronounced sensitivity to the differential input voltage ($[+v_{in}]$ - $[-v_{in}]$) has been noted for comparators ([123],[127]). With voltage comparators, large (rail-to rail) voltage swings are often generated [125] and these last for several µs. In operational amplifiers the range of amplitudes is wider but high LET ions can generate transients of several volts amplitude. The size of the transient tends to increase linearly with deposited charge until saturation is reached [131].

In only two cases [131] has device modelling been used to determine the critical charge for transient generation. This was for the LM124 amplifier and LM111 comparator and a value ~ 1pC was derived. This can be deposited by a variety of ions (a threshold LET of 1-2 MeV.cm^2/mg was found) because of the large depth over which charge can be collected in a bulk device (the authors estimated 30-100 µm). Typical charge deposition times are ~ 10ns [126], though the circuit response of a device is expected to be more dependent on the total charge collected than the details of the charge generation waveform [131].

It is usual to define the voltage level (or levels) at which to count a transient as an 'event' and to define a cross section, σ in the usual way:

$$\sigma = N/(\phi \cos\theta) \tag{24}$$

where ϕ is the fluence, θ the angle of incidence and N the number of events (which will depend on the threshold for detection of a transient). On-orbit predictions of event rates can then be determined as for SEUs (section 2.2).

It is important to be able to determine the size of events that will occur in complete circuits rather than in discrete devices since the transients will be modified by external components such as amplifiers and filters, however a simulator for the generation of transients at a device output is first required.

Detailed 'ab initio' device level simulations have been carried out for the LM111 and LM124 devices and the mechanisms and sensitive device junctions identified. For these devices the SPICE circuit model was detailed at the transistor level using manufacturers data and reverse engineering of the die. However it is not a simple task to re-run the simulations for a variety of circuit configurations. It would not be feasible to perform these investigations except in special

circumstances because the device layout information is not available. Instead the equivalent circuit SPICE model is all that can be used.

It would be desirable if a SPICE model could be derived which would simulate transient events at the device output - which could then be incorporated into a SPICE model for a complete circuit. A disadvantage is that pulses can generally only be applied to a device input since intermediate (e.g. gain) stages are often simulated in SPICE models using voltage controlled current sources [134] and so the intermediate transistors are not usually accessible. In the case of operational amplifiers, the input stages are often the most sensitive or else has comparable sensitivity with later stages. With some comparators the sensitive stage will depend on biasing. For example the LM139 output becomes decoupled from the input stage at high differential input voltage and other internal nodes become dominant [127]. Hence we can expect a simple 'add-on' SPICE transient generator applied to the device inputs to be not as applicable for comparator devices.

Two types of SPICE 'add-on' transient generator were considered: a transient voltage controlled current source and a switched capacitor, which is charged from a switched voltage source. Both, in effect, deliver a charge pulse to the input pin(s) of a device. The transient voltage output was then observed on the device output. The core of the SPICE code is freely available to users however specific implementations are available from vendors. For this study the B2 SPICE A/D 2000 software from Beige Bag Software Inc. [135] was used. This is a low cost, fully functional, mixed mode package with easy to use schematic entry.

Figures 5 to 8 show the circuit diagrams for typical amplifier and comparator simulations. The following amplifiers were simulated:

- OP07
- OP37
- OP15
- LM124
- LM218
- CLC426

and the LM111 and LM339 comparators.

For the amplifiers it was found that the two approaches, current source and switched capacitor, gave very similar transient outputs. This is not surprising since it is showing that the response of the device is slower than the 10ns timescale of the input pulse. This is illustrated in figures 9 to 14. The current source is more convenient to use as a transient source since convergence is easier to achieve and the switched capacitor source tends to be sensitive to the off-resistance of the switches (which needs to be ~ 10^{12} Ohms). The OP07, OP15 and LM124 are slow amplifiers and so it is not surprising that the transients are of longer duration then for the faster LM108, LM218, CLC426 and OP37 amplifiers (the OP37 results are similar to the other fast amplifiers and so are not shown).

It is seen that output transients can be generated with the required range of amplitudes and pulse widths. Typical input charge pulses were ~ 10-50 pC. For the amplifiers, the output transient shapes were sensitive to the gain resistors (input and feedback) used in the amplifier for small input transients but not once the output transients had reached saturation (i.e. for large input pulses). As might be expected, a higher amplifier gain results in larger transients at the output. In some cases there is also a sensitivity to the absolute values of the resistors. Although, a sensitivity to resistor values has been noted, no systematic experimental

investigation has been carried out. It is suggested that SPICE simulations, as performed here, would be a useful precursor to experimental measurements so as to gauge the sensitivity to experimental parameters - although it has to be emphasised that the technique suffers from the limitations discussed above (particularly the inaccessibility of individual junctions and internal transistors).

Figure 15 shows simulation results for the LM111 and LM339 comparators. Only the 0V differential input condition gave output transients, presumable because, as mentioned above, the SPICE model is not representing the internals of the device. However large transients can be demonstrated as expected.

One of the main benefits of SPICE modelling is to examine the effect of external circuits. As mentioned by Harboe-Sorensen et al. [124], simple addition of a 100n capacitor can often be effective in suppressing transients. This is illustrated in figures 16 and 17 which show results for the OP15 and LM218 amplifiers. .In the latter case, a series 10R resistor was also needed to stop the (fast) amplifier from oscillating. A 100n capacitor was similarly effective in removing transients from the LM111 and LM339 waveforms.

Another method of analysing the effect on external circuits would be simply to use a voltage transient source (voltage controlled voltage source) directly at the device output. A conservative case would be to take a rail-rail amplitude (or perhaps just less than rail-rail since SPICE may not accurately model the saturated condition in some cases) and ~ 4 μs duration (e.g. a sharp rise and exponential tail). Only if the circuit shows an undesirable response to this 'worst case' transient would a more accurate simulation (or better, still, representative experimental measurements) be needed. This is the approach recently advocated by Marec et al. [136]. Ideally, it would be better to have a database of worst-case transients for each device type which could be applied to the circuit model, however this is not available at the present time. Poivey et al. [132] have pointed out that "extensive testing with a large variety of test parameters and conditions is needed in order to bound the different worst case responses", particularly for operational amplifiers.

Conclusion: **Use of simple 'add-on' SPICE transient pulse generators can give representative transients at device outputs, particularly for operational amplifiers. For voltage comparators the technique does not simulate the dependence of heavy ion transients on differential input voltage which is seen experimentally but this is to be expected as pulses cannot be applied to the sensitive internal nodes which pertain at high differential input voltages. The SPICE method can be used as a precursor to device testing and to gauge the effect of external circuitry (e.g. filter capacitors). It has to be emphasised however that simple SPICE modelling cannot fully simulate the complex interactions, which occur in a real device and so can only be used as a rough guide.**

A recommended technique is simply to use a large amplitude voltage transient (either near-rail-rail, or previously established worst case) at the device output and to perform detailed analysis (or experimental measurements) only if unwanted effects are seen.

Another alternative could be to irradiate a device 'in situ' in the circuit, e.g. using a 200 MeV proton beam.
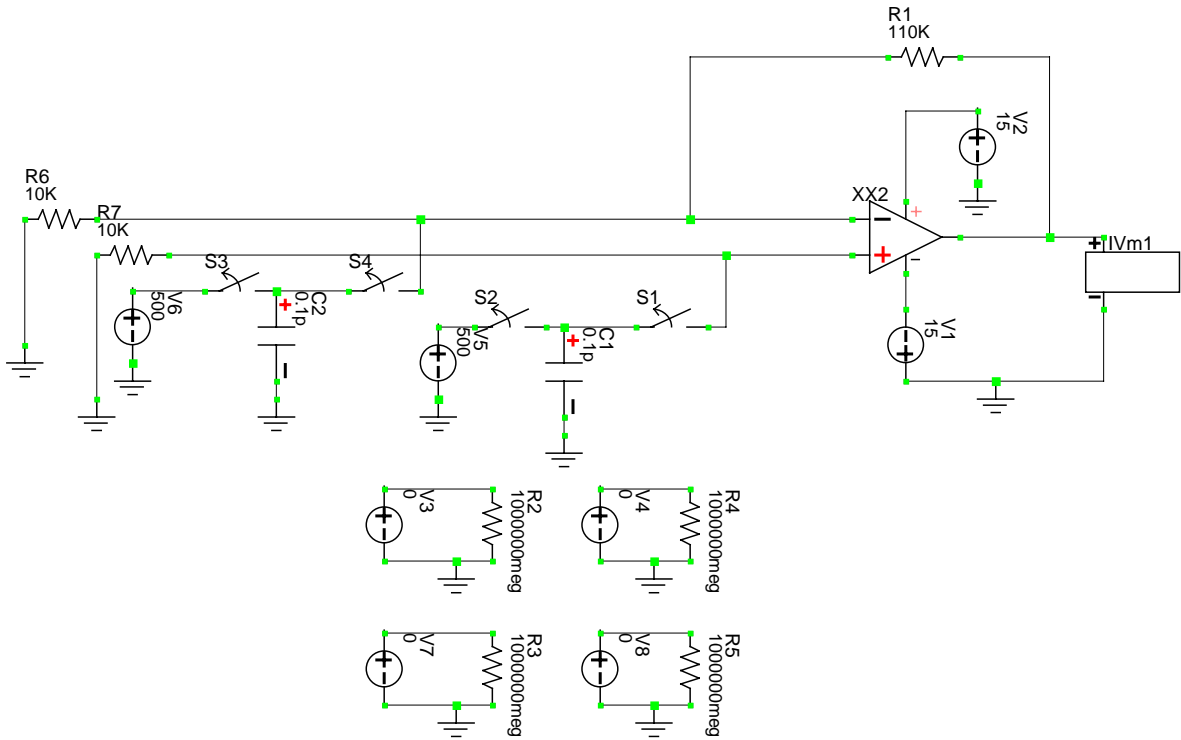
Figure 5 Circuit diagram for simulating transient events in an amplifier using switched capacitor transient inputs. The voltage sources at the bottom of the picture define the operation of the switches, which typically had 10 ns opening times.
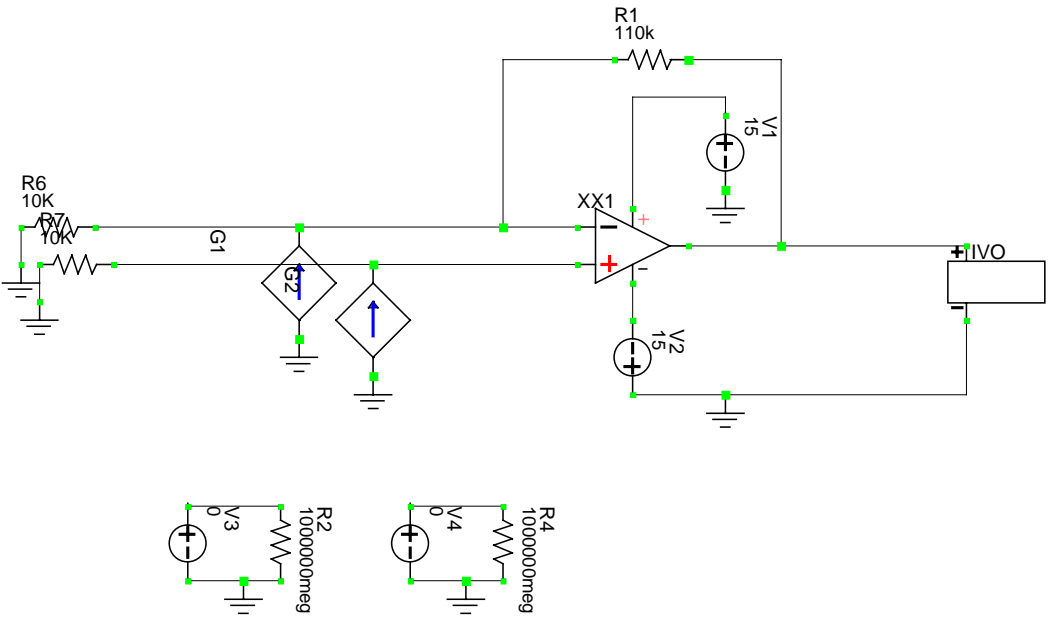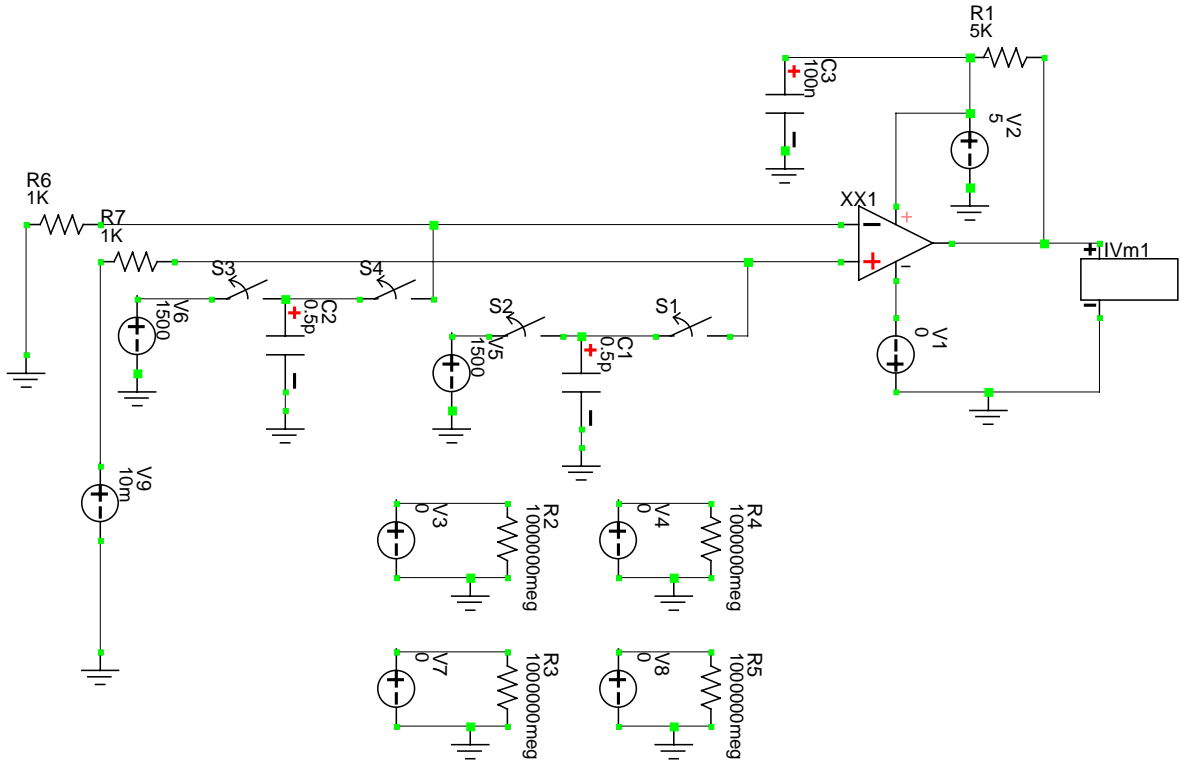

Figure 6 Circuit diagram for simulating transient events in an amplifier using voltage controlled current source inputs. The voltage sources at the bottom of the picture define the transient operation of the sources. Typically a 10ns linear turn-on and -off time and 10 ns duration was used with a peak current of between 1.8 mA and 20 mA depending on the amplifier used

Figure 7 Circuit diagram for simulating transient events in an comparator using switched capacitor transient inputs. The voltage sources at the bottom of the picture define the operation of the switches, which typically had 10 ns opening times
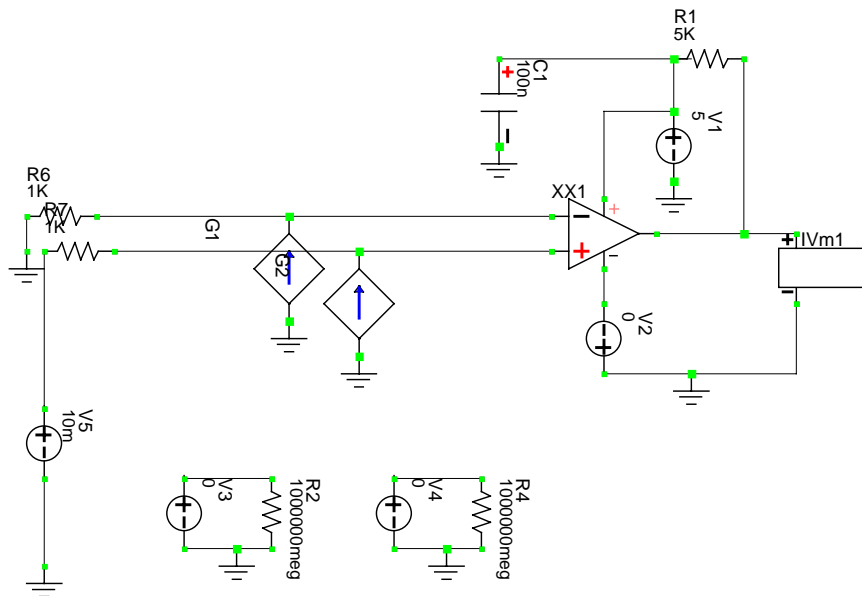
Figure 8 Circuit diagram for simulating transient events in a comparator using voltage controlled current source inputs. The voltage sources at the bottom of the picture define the transient operation of the sources. Typically a 10ns linear turn-on and -off time and 10 ns duration was used with a peak current of between 1.8 mA and 20 mA depending on the amplifier used
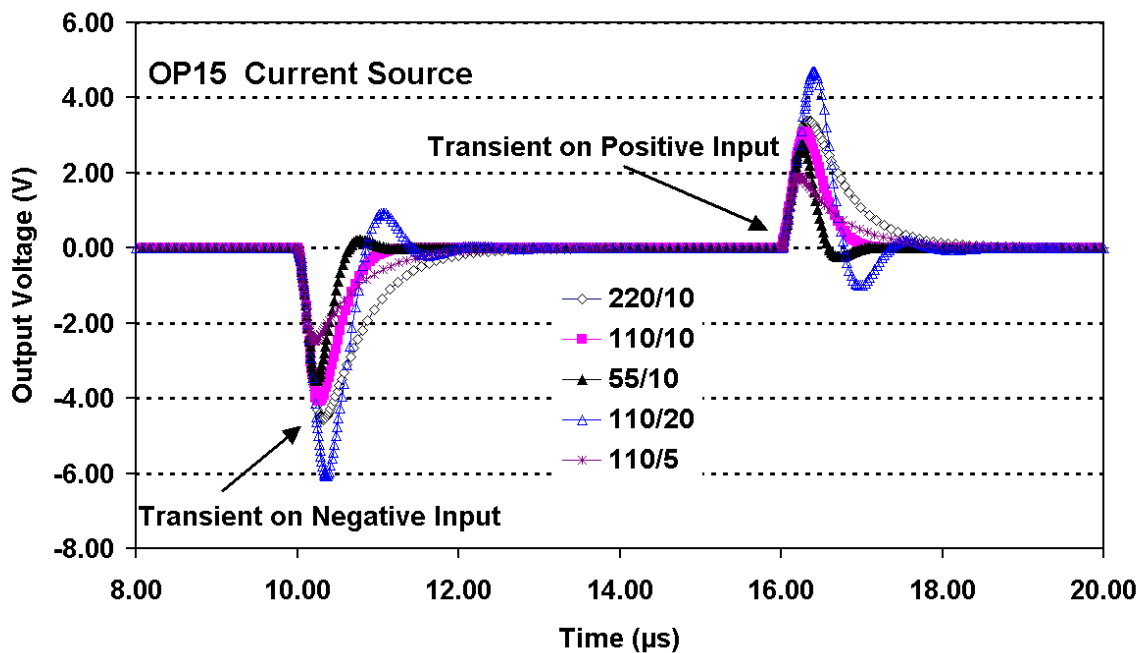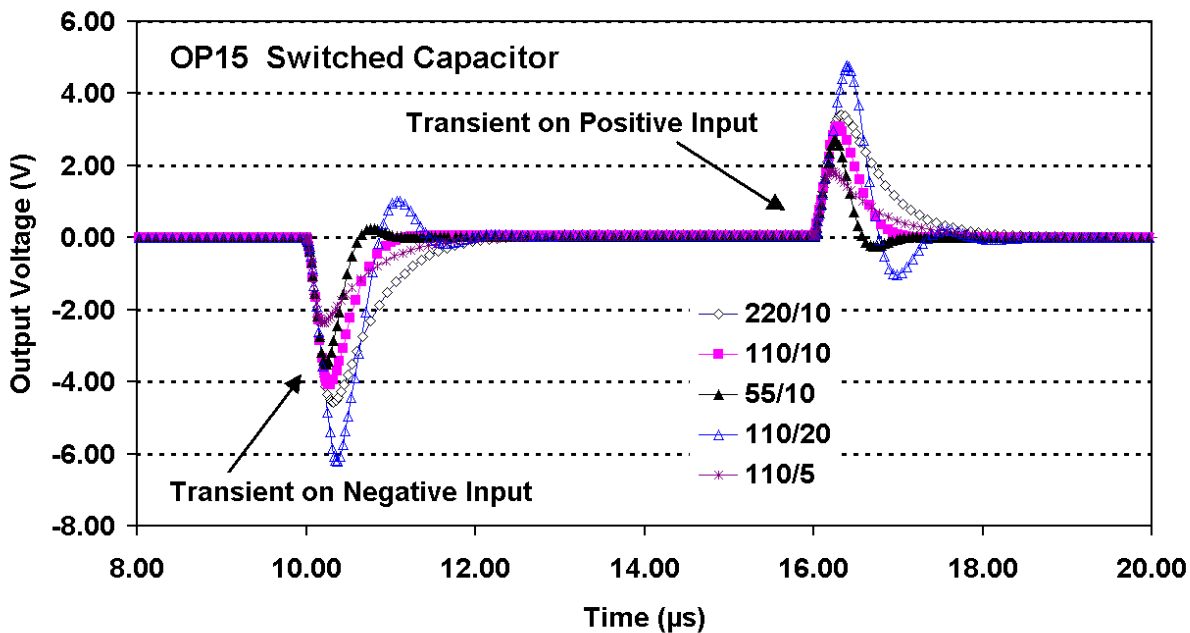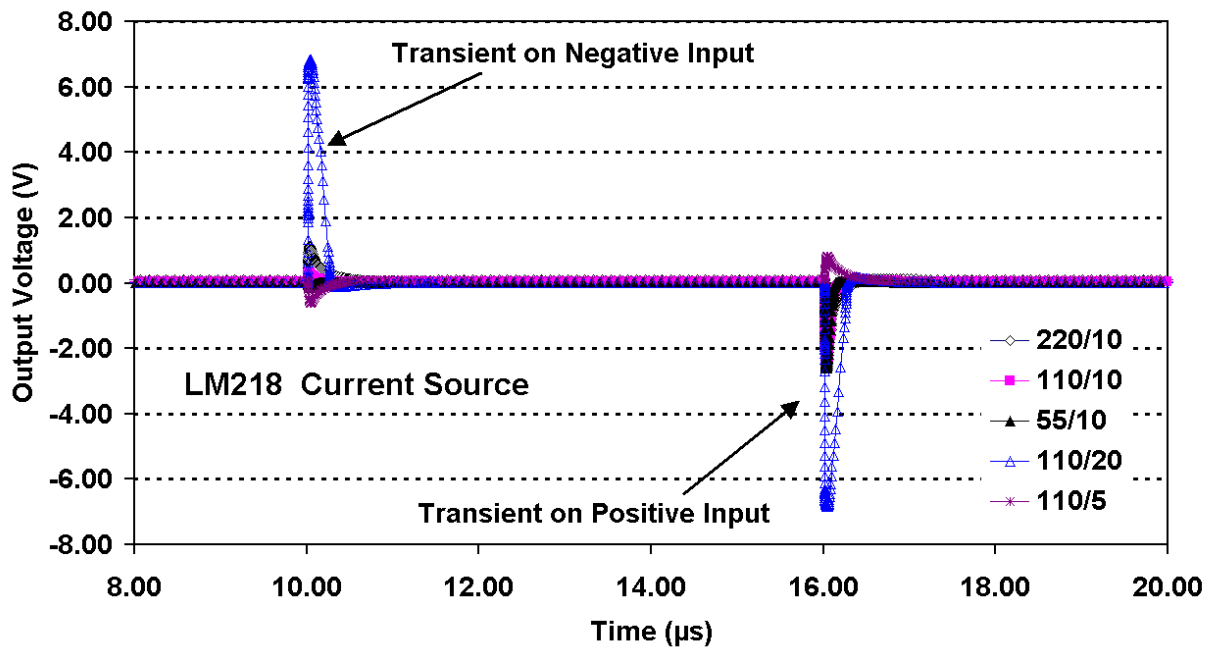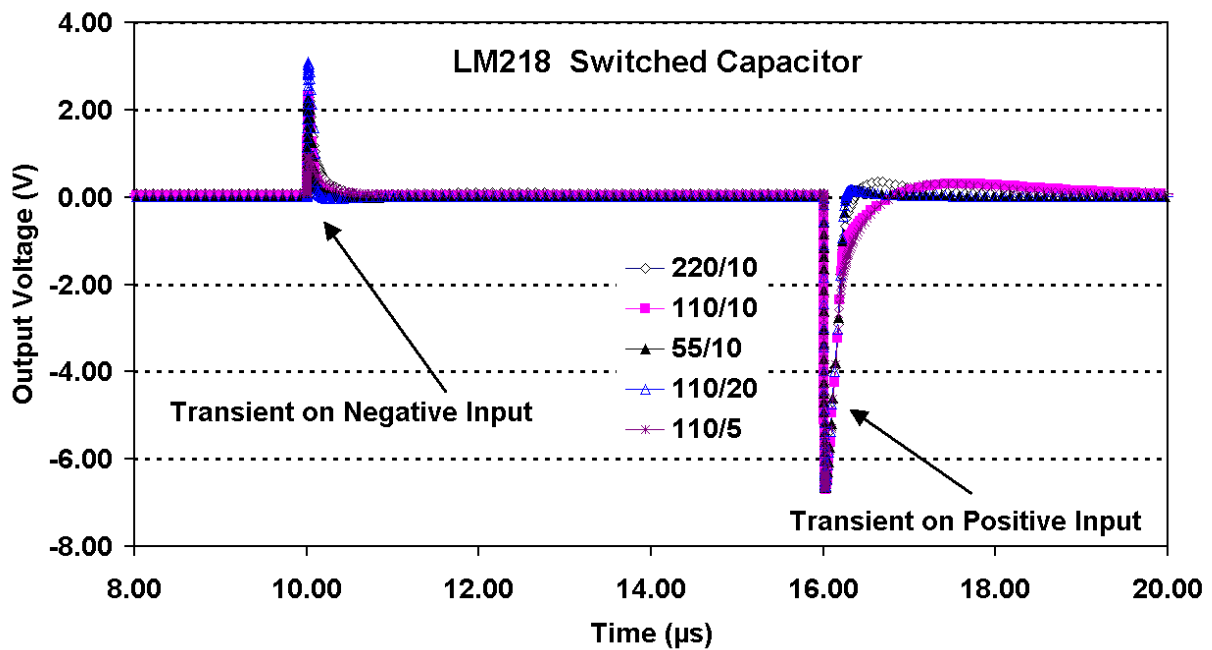
Figure 9 PSPICE transient simulations for the OP15 amplifier. Positive and negative transients were applied to the device inputs at 10 and 16 μs. The plots are labeled with the feedback/input resistor values (in k Ohms)

Figure 10 PSPICE transient simulations for the LM218 amplifier. Positive and negative transients were applied to the device inputs at 10 and 16 µs. The plots are labeled with the feedback/input resistor values (in k Ohms)
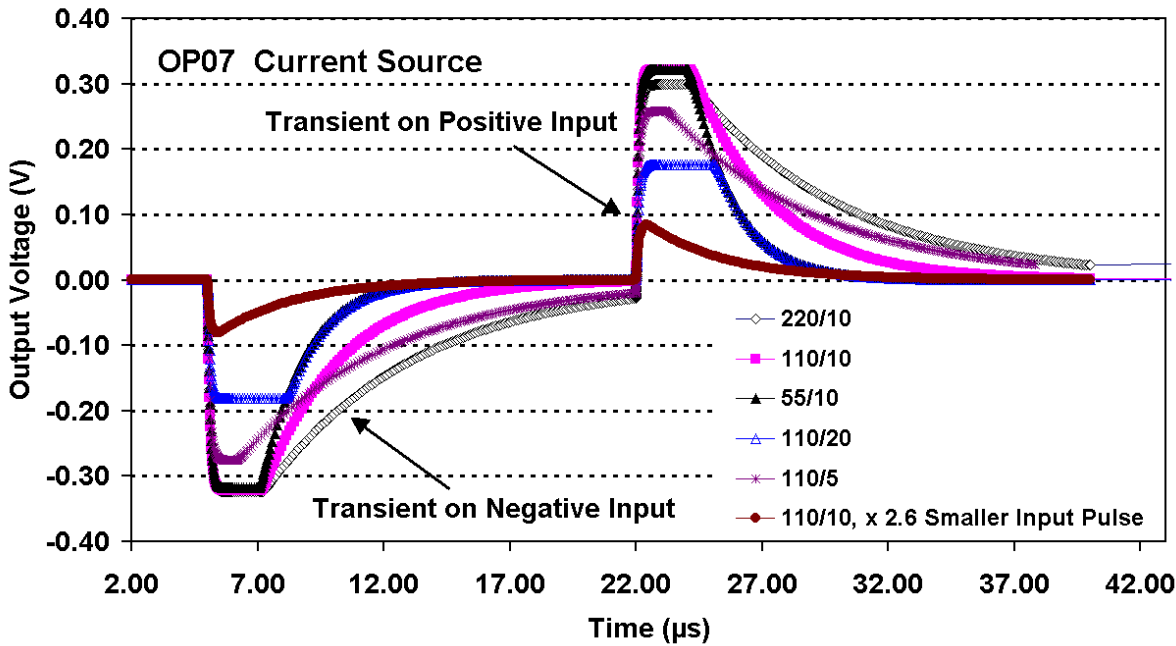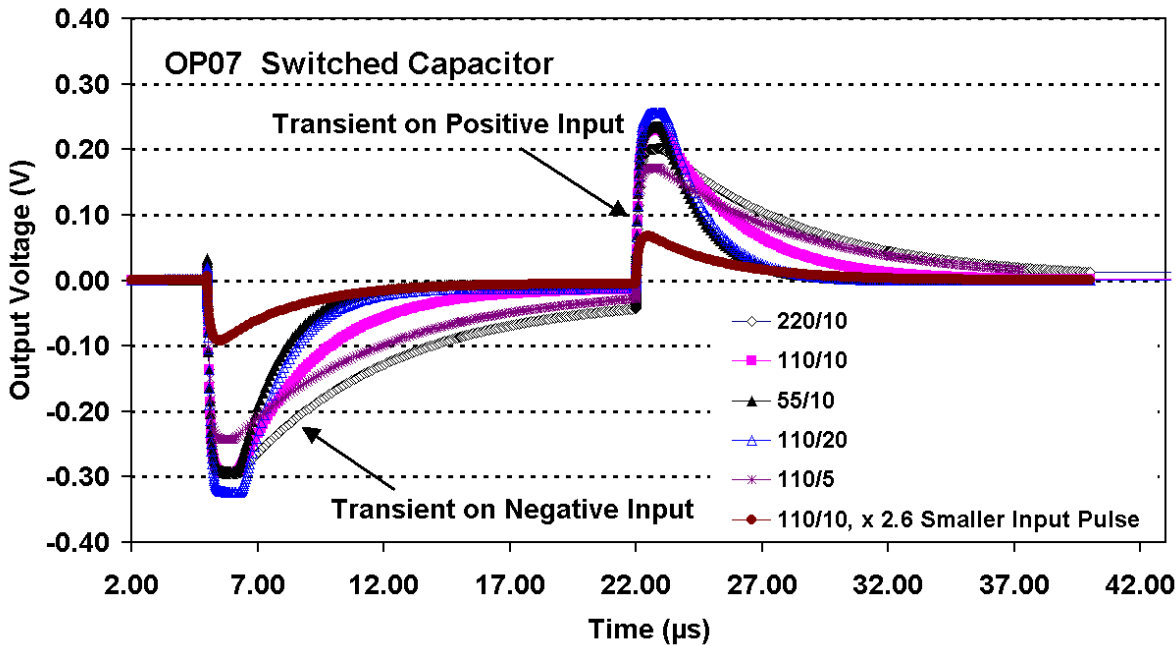
a)

b)

Figure 11 PSPICE transient simulations for the OP07 amplifier. Positive and negative transients were applied to the device inputs at 5 and 22 µs. The plots are labeled with the feedback/input resistor values (in k Ohms)

Figure 12 PSPICE transient simulations for the CLC426 amplifier. Positive and negative transients were applied to the device inputs at 10 and 16 µs. The plots are labeled with the feedback/input resistor values (in k Ohms)

Figure 13 PSPICE transient simulations for the LM124 amplifier. Positive and negative transients were applied to the device inputs at 10 and 22 µs. The plots are labeled with the feedback/input resistor values (in k Ohms)
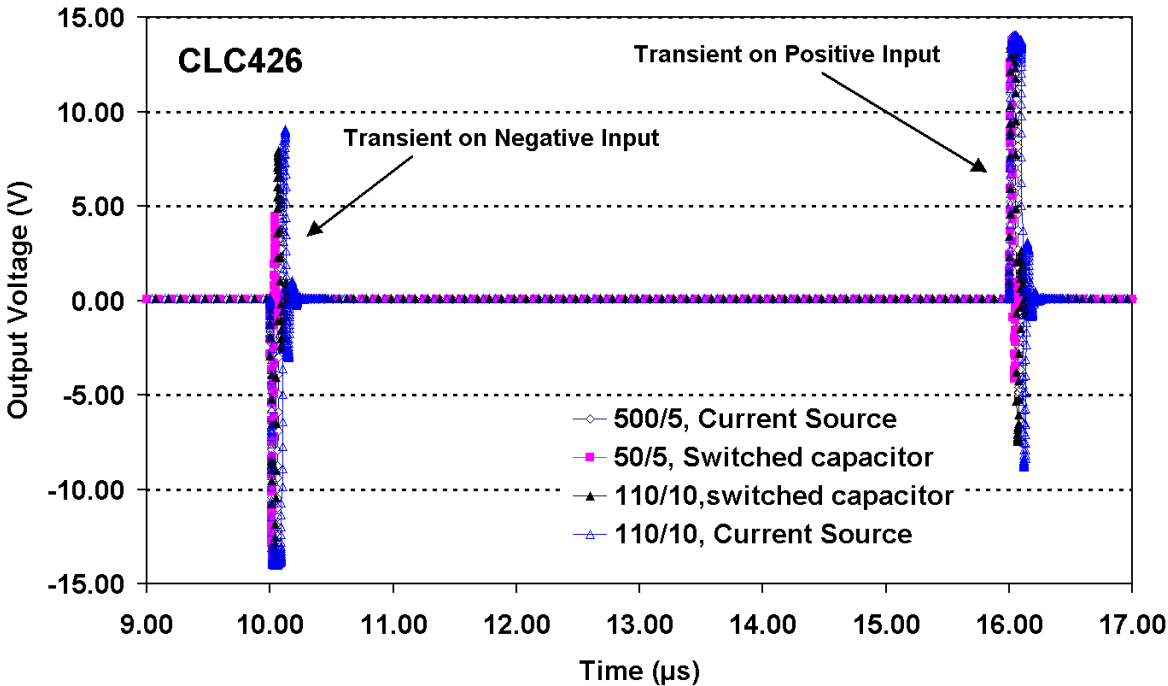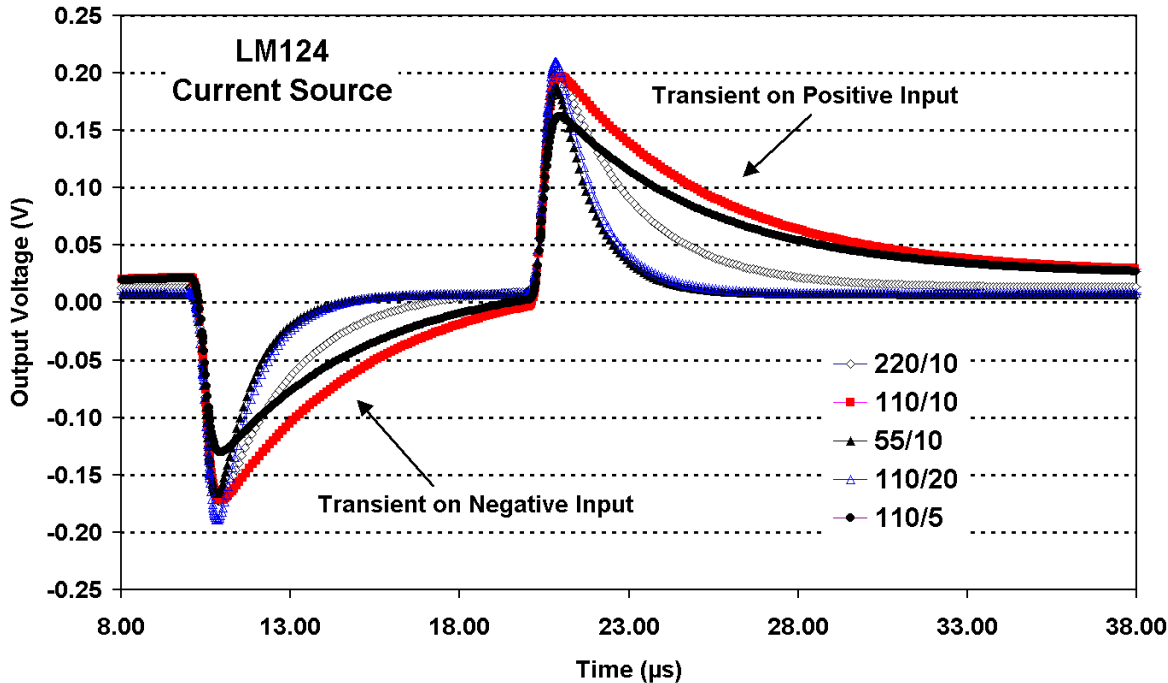
Figure 14 PSPICE transient simulations for the LM108 amplifier. Positive and negative transients were applied to the device inputs at 10 and 16 µs. A 110 k feedback resistor and 10 k input resistors were used.
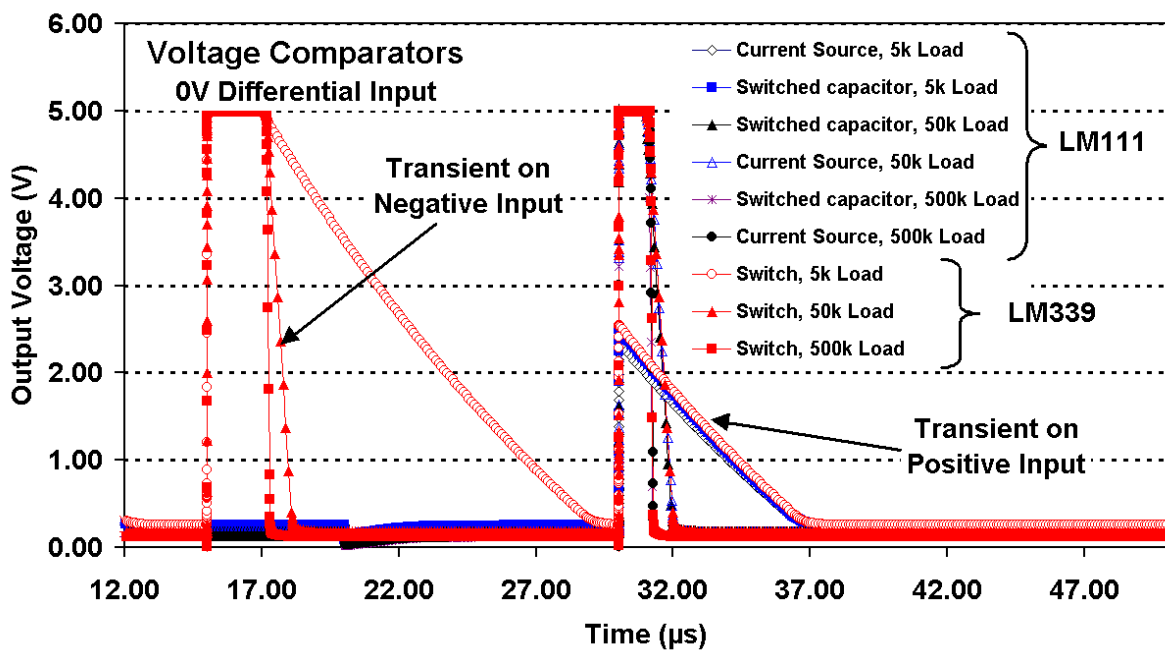
Figure 15 PSPICE transient simulations for the LM111 and LM339 voltage comparators. Positive and negative transients were applied to the device inputs at 15 and 20 µs. The plots are labelled with the load resistor values (in k Ohms)
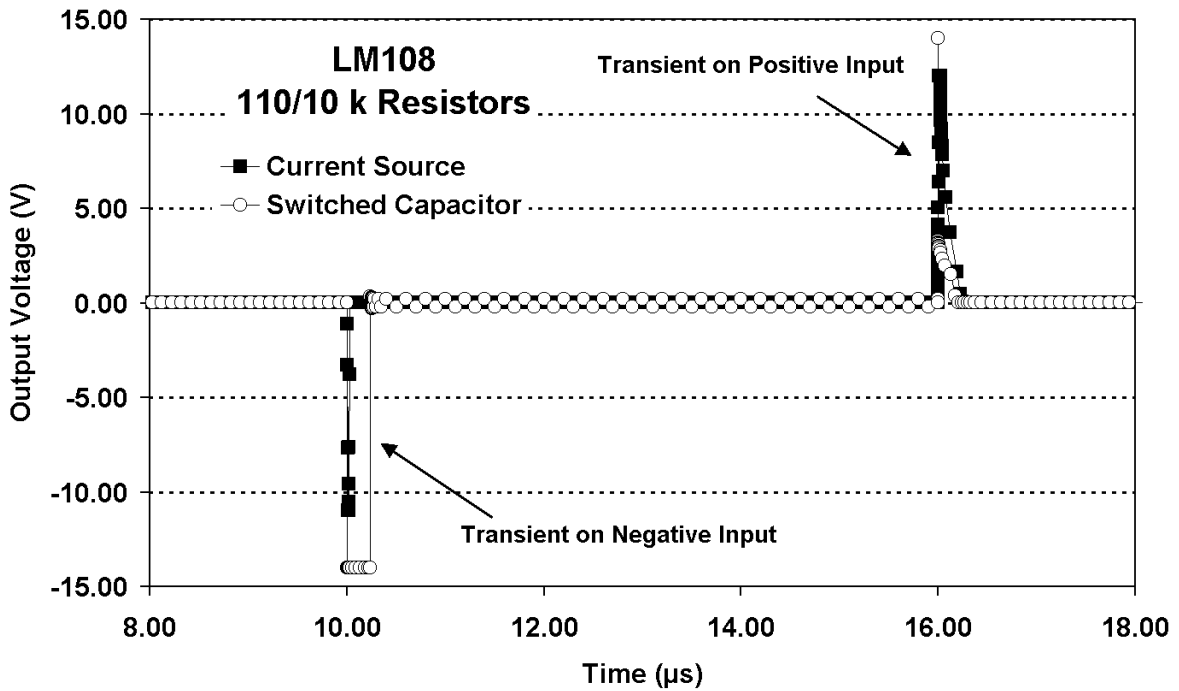
Figure 16 PSPICE transient simulations for the OP15 amplifier with and without a 100n capacitor at the output

Figure 17 PSPICE transient simulations for the LM218 amplifier with and without a 100n capacitor at the output (and 10R series resistor)

2.8 TRANSIENT EFFECTS IN OPTOCOUPLERS AND FIBRE-OPTIC LINKS

Transient effects in opto-couplers and fibre optic data links have been reviewed by Marshall et al. [137]. In both cases the most sensitive element for single event upset is th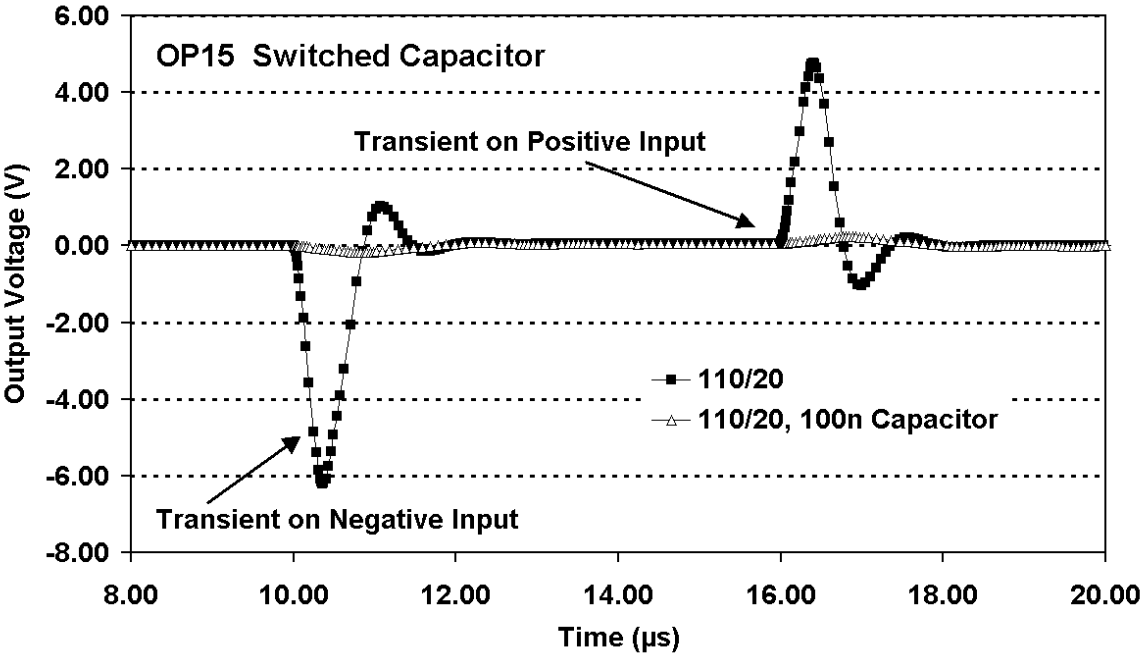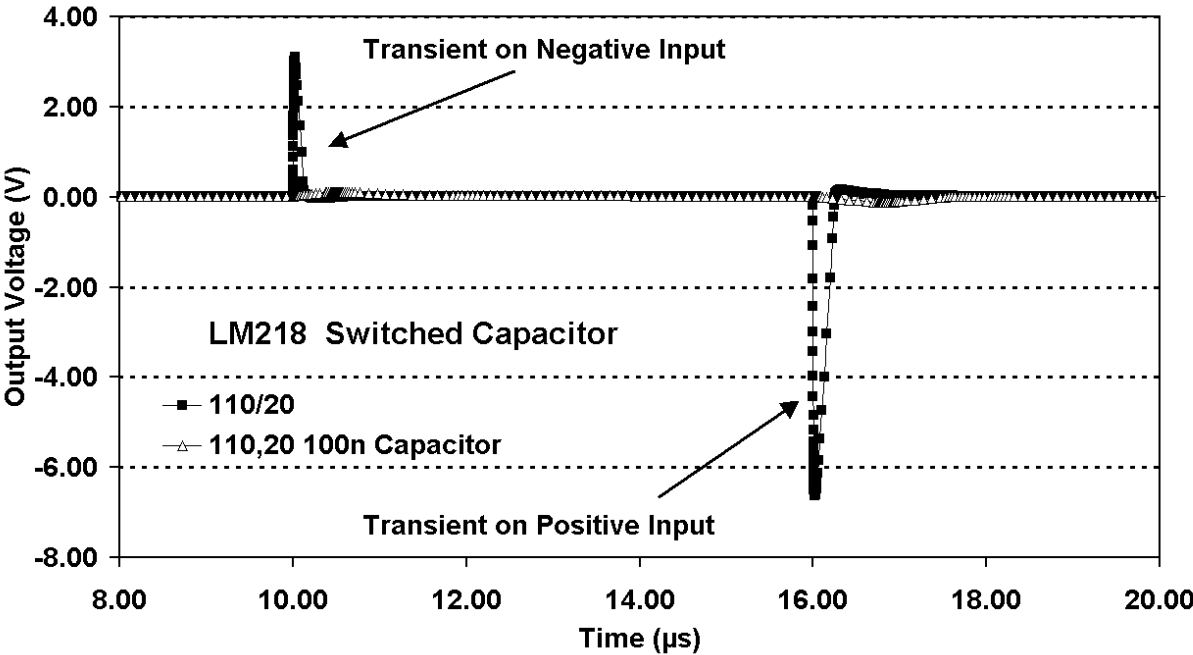e photodetector. This is because the optical signal typically has low power and the electrical signal, which represents a single bit is normally 100-1000 electrons and is easily corrupted by even lightly ionizing particles that strike the detector (which typically has a diameter of several hundred microns).

In [138] the experimental bit error cross section for fibre links was interpreted in terms of direct proton ionization and the conclusion was that error rates can be calculated using the path length distribution and calculations as in CREME-96 [24]. However there is some doubt that the PUP routine in CREME-96 is correct for protons, which stop in the material.

Error rate prediction for optocouplers is not as advanced as for fibre links. Johnston et al [139] have shown that the error cross section depends on angle of incidence and proton energy (LET) for protons. The authors make the suggestion to empirically determine an effective cross section at a given proton energy by integrating the cross section over all arrival angles and establishing an average cross section for a given proton energy. By measuring the angular dependence over the necessary range of energies, and determining the appropriate "effective" cross section dependence on energy, the cross section data could be combined with proton spectra to arrive at an empirically based effective rate. This approach may be suited for some applications but a large amount of experimental data is needed. As an alternative, Marshall et al [137] have suggested an 'effective LET' approach.

Conclusion: **In principle, SEU rate prediction for fibre optic data links and optocouplers can be made using the formalism for SEU prediction discussed in section 2.2. However care has to be taken to include the angular and energy dependence of proton effects for optocouplers. Modifications to error rate prediction models for optocouplers (e.g. based on CREME96) may be needed in future once a formalism has been accepted.**

2.9 DOSE ENHANCEMENT EFFECTS

Dose enhancement occurs in electron and bremsstrahlung environments where high-Z (i.e. high atomic number) materials overlay or are close to the SiO_2 layer of a device. The enhancement comes about from departures from radiation equilibrium at an interface with a high-- coating [140] or from backscatter of Compton electrons (generated by bremsstrahlung) or reflection of electron flux from high-Z layers [141,142]. High-Z materials can be gold coatings, package materials (such as Kovar, gold-plated kovar or high Z ceramics) or high-Z solder bump-bonds and beam-leads.

Solin [141,142], used the CEPXS/ONEBFP to estimate the dose enhancement factor due to electron scattering. The worst case occurs when a device is lightly shielded on the side opposite the high-Z material so that there is a light-shielding/oxide/high-Z/heavy-shielding geometry. Enhancement factors can be an order of magnitude in high electron environments

(such as GEO).   Experimental measurements of dose enhancement for various package materials have been made by Brucker et al. [143], who found similar values.

For dose enhancement studies, other codes exist (such as ITS, EGS).   However there are significant run time and statistics problems that deterministic codes such as CEPXS overcome.

Conclusion: **Accurate estimation of dose enhancement effects in high electron environments needs a particle transport code, which can calculate electron and bremsstralung fluxes (and the ionising dose produced) for arbitrary shielding geometries which include high Z layers.**

2.10   MICRODOSE EFFECTS

Oldham et al [144] showed that a single heavy ion can deposit enough dose in the gate oxide above the small sensitive volume of a high density memory to cause a localized total dose failure (otherwise known as a single Hard error, SHE, or a 'stuck bit').   Stuck bits can also be produced by single event gate rupture.   In modern devices the error rate for stuck bits has remained low, probably because of architecture changes and the use of thin gate oxides. However microdose effects still pose a potential threat, particularly for mass memories (DRAMS).   Edmonds et al. [145] have recently shown that a stuck bit cross section can be defined for some DRAMs which is independent of particle fluence.   That is, the effect behaves "linearly" and an event cross section can be determined unambiguously.   However this does not apply to devices where the effect depends on the previous dose history (as in the example given by Dufour et al. [146]).

Edmonds et al. have noted that the angular dependence of the stuck bit cross section has not yet been studied in detail and also that stuck bits created by microdose can be affected by annealing.

Pickel [147] has suggested that microdose effects may become important for high density CMOS readout circuits for infrared focal plane detector arrays.

Conclusion: **A tool for predicting energy deposition in small volumes could also be used to investigate the likelihood of experiencing single hard errors in MOS circuits.**

2.11 EFFECTS IN DETECTOR CRYSTALS FOR SPACE SCIENCE APPLICATIONS

Charge-deposition spectra of ionising radiation in detector materials is a major source of background in astronomy and astrophysics missions ranging from the infrared to the gamma ray. In the latter case the contribution of radioactivity limits sensitivity even outside the regimes of intense particle radiation [148]. Extensive work has been performed on NaI, CsI, bismuth germanate and germanium but further calculations are required for newer materials, such as gadolinium oxyothosilicate, cadmium zinc telluride, barium fluoride. The use of heavy spacecraft and detector systems necessitates the accurate computation of secondary radiation and its spectrum. In modelling activation, there is a need for an optimised technique for producing spallation product and response function libraries.

Use of compound semiconductors for high-energy astrophysics missions has recently been discussed by Bavdaz et al. [149]. CdZnTe is a material, which is starting to be considered for space applications. However Hull et al [150] have pointed out that the material is prone to radiation-induced carrier (in this case electron) trapping - much more so than hole trapping in germanium (which is commonly used for gamma ray detection), even though CdZnTe crystals intrinsically suffer from high defect levels. More work on device characterisation is needed, however, before specific requirements on analysis tools can be derived.

Conclusion: **The main need for space science detectors is at present judged to be the calculation of secondary spectra from shielding materials. In modelling activation of detector materials there is a need for an optimised technique for producing spallation product and response function libraries.**

3.   REFERENCES

[1]   Available on-line at http://www.spenvis.oma.be

[2]   Available on-line at http://www.techcentreuk.power.alstom.com/

[3]   G. P. Summers, E. A. Burke, P. Shapiro and S. R. Messenger, "Damage correlations in semiconductors exposed to gamma, electron and proton radiations", IEEE Trans. Nucl. Sci., vol. 40(6), pp. 1372-1379, 1993.

[4]   C. J. Dale, L. Chen, P. J. McNulty, P. W. Marshall, and E. A. Burke, "A comparison of Monte Carlo and analytic treatments of displacement in Si microvolumes", IEEE Trans. on Nucl. Sci., vol. 41, no. 6, pp. 1974-1981, Dec. 1994.

[5]   I. Jun, "Effects of secondary particles on the total dose and the displacement damage in space proton environments", IEEE Trans. on Nucl. Sci., vol. 48, no. 1, pp. 162-175, Feb. 2001.

[6]   M. Alurrade, M. Victoria, A. Caro and D. Gavillet, "Nuclear and damage effects in Si produced by irradiations with medium energy protons", IEEE Trans. on Nucl. Sci., vol. 38, no. 6, pp. 1210-1215, Dec. 1991.

[7]   A. Akkerman, J. Barak, M. B. Chadwick, J. Levinson, M. Murat and Y. Lifshitz, "updated NIEL calculations for estimating the damage induced by particles and γ rays in Si and GaAs", Radiation Physics and Chemistry, vol. 62, pp. 301-310, 2001

[8]   S. R. Messenger, E. A. Burke, R. J. Walters, G. P. Summers and M. A. Xapsos, "NIEL and damage correlations for high energy protons in Gallium Arsenide devices", IEEE Trans. Nucl. Sci., 48(6), pp. 2121-2126, Dec. 2001.

[9]   R. J. Walters, G. J. Shaw, G. P. Summers, E. A. Burke and S. R. Messenger, "Radiation effects in $Ga_{0.47}In_{0.53}As$ devices", IEEE Trans. on Nucl. Sci., vol. 39, no. 6, pp. 2257-2264, Dec. 1992.

[10]   P. W. Marshall, C. J. Dale, G. P. Summers, E. A W E. A. Burke, "Proton, neutron and electron induced displacement damage in germanium", IEEE Trans. on Nucl. Sci., vol. 36, no. 6, pp. 1882-1889, Dec. 1989.

[11]   P. F. Hinrichsen, A. J. Houdayer, A. L. Barry and V. J. Vincent, "Proton induced damage in SiC light emitting diodes", IEEE Trans. on Nucl. Sci., vol. 45, no. 6, pp. 2808-2812, Dec. 1998.

[12]   S. R. Messenger, E. A Burke, G. P. Summers, M. A. Xapsos, R. J. Walters, E. M.; Jackson, and B. D. Weaver, " Nonionizing energy loss (NIEL) for heavy ions", IEEE Trans. on Nucl. Sci., vol. 46, no. 6, pp. 1595 -1602, Dec. 1999.

[13]   B. G. Rax, C. I. Lee, A. H. Johnston and C. E. Barnes, "Total dose and proton damage in optocouplers", IEEE Trans. on Nucl. Sci., vol. 43, no. 6, pp. 3167-3173, Dec. 1996.

[14]   G. R. Hopkinson, "Proton-induced changes in CTE for n-channel CCDs and the effect on star tracker performance", ", IEEE Trans. on Nucl. Sci., vol. 47, no. 6, pp. 2460-2465, Dec. 2000.

[15]   A. Ruzin, G. Casse, M. Glaser, A. Zanet, F. Lemeilleur and S. Watts, "Comparison of radiation damage in silicon induced by proton and neutron irradiation", IEEE Trans. on Nucl. Sci., vol. 46, no. 5, pp. 1310-1313, Oct. 1999.

[16]   C. Dale, P. Marshall, B. Cummings, L. Shamey and A. Holland, "Displacement damage effects in mixed particle environments for shielded spacecraft CCDs", IEEE Trans. on Nucl. Sci., vol. 40, no. 6, pp. 1628-1637, Dec. 1993.

[17]   R. J. Walters, S. R. Messenger, H. L. Cotal, G. P. Summers and E. A. Burke, "Electron and proton irradiation-induced degradation of epitaxial InP solar cells", Solid State Electronics, vol. 39(6), pp. 797-805, 1996.

[18]   R. A. Reed, P W Marshall, C. J. Marshall, R. L. Ladbury, H. S. Kim, L. X. Nguyen, J. L. Barth, and K. A. LaBel, "Energy dependence of proton damage in AlGaAs light-emitting diodes," IEEE Trans. Nucl. Sci., vol. 47(6), pp. 2492-2499, Dec. 2000.

[19]   R.J. Walters, S.R. Messenger, G.P. Summers, E.A. Burke, S.M. Khanna, D. Estan, L.S. Erhardt, H.C. Liu, M. Gao, M. Buchanan, A.J. SpringThorpe, A. Houdayer, and C. Carlone, "Correlation of Proton Radiation Damage in InGaAs/GaAs Quantum Well Light Emitting Diodes", IEEE Trans. Nucl. Sci., 48(6), pp. 1773-1777, Dec. 2001.

[20]   A. H. Johnston and T. F. Miyahira, "Characterization of proton damage in light-emitting diodes," IEEE Trans. Nucl. Sci., vol. 47(6), pp. 2500-2507, Dec. 2000.

[21]   I. Jun and W. McAlpine, "Displacement damage in silicon due to secondary neutrons, pions, deuterons and alphas from proton interactions with materials", IEEE Trans. Nucl. Sci., 48(6), pp. 2034-2038, Dec. 2001.

[22]   E. Petersen, "Single-event analysis and prediction", Short Course Notes, ch. III, IEEE Nuclear and Space Radiation Effects Conference, Snowmass, 21 July 1997.

[23]   SPACE RADIATION code (J. Letaw, Severn Communications Corporation, 1989)

[24]   http://crsp3.nrl.navy.mil/creme96/

[25]   J. B. Langworthy, "Depletion region geometry analysis applied to single event sensitivity", IEEE Trans. Nucl. Sci., vol 36(6), pp. 2427-2434, Dec. 1989.

[26]   W. L. Bendel and E. L. Petersen, "Proton upsets in orbit", " IEEE Trans. Nucl. Sci., vol 30(6), pp. 4481-4485, Dec. 1983.

[27]   E. L. Petersen, "The SEU figure of merit and proton upset rate calculations", IEEE Trans. Nucl. Sci., vol 45(6), pp. 2550-2562, Dec. 1998.

[28]   J. Barak, "Empirical modelling of proton induced SEU rates", IEEE Trans. Nucl. Sci., vol 47(3), pp. 545-550, Jun. 2000.

[29]   P. Calvel, C. Barillot, P. Lamothe and R. Ecoffet, "An empirical model for predicting proton induced upset", IEEE Trans. Nucl. Sci., vol. 43(6), pp. 2827-2832, Dec. 1996.

[30]   J. Barak, "Analytical microdosimetry model for proton induced SEU in modern devices", IEEE Trans. Nucl. Sci., 48(6), pp. 1937-1945, Dec. 2001..

[31]   F. Wrobel, J.-M. Palau, M-C. Calvet O. Bersillon and H. Duarte, "Incidence of multi-particel events on soft error rates caused by n-Si nuclear reactions", IEEE Trans. Nucl. Sci., vol. 47(6), pp. 2580-2585, Dec. 2000.

[32]   G. J. Hoffman, R. J. Peterson, C. J. Gelderloos, R. A. Ristinen, M. E. Nelson, A. Thompson, J. F. Ziegler and H. Mullfield, "Light-hadron induced SER and scaling relations for 16- and 64-Mb DRAMS", IEEE Trans. Nucl. Sci., vol. 47(2), pp. 403-407, Apr. 2000.

[33]   S. Buchner, A. B. Campbell, T. Meehan, K. A. Clark, D. McMorrow, C. Dyer, C. Sanderson, C. Comber and S. Kuboyama, "Investigation of single-ion multiple-bit upsets in memories on board a space experiment", IEEE Trans. Nucl. Sci., vol. 47(3), pp. 705-711, Jun 2000.

[34]   C. S. Dyer, C. Comber, P. R. Truscott, C. Sanderson, C. Underwood, M. Oldfield, A. Cambell, S. Buchner and T. Meehan, "Microdosimetry code simulation of charge deposition spectra, single event upsets and multiple-bit upsets", IEEE Trans. Nucl. Sci., vol. 46(6), pp. 1486-1493, Dec. 1999.

[35]   G. M. Swift and S. M. Guertin, "In-flight observations of multiple-bit upset in DRAMs", IEEE Trans. Nucl. Sci., vol 47(6), pp. 2386-2391, Dec. 2000.

[36]   F. Wrobel, J-M. Palau, M-C. Calvet O. Bersillon and H. Duarte, "Simulation of downscaling effects on multiple bits upsets induced by nucleons", IEEE Trans. Nucl. Sci., 48(6), pp. 1946-1952, Dec. 2001.

[37]   R. Harboe-Sorensen, E. Daly, F. Teston, H. Schweitzer, R. Nartallo, P. Perol, F. Vandenbussche, H. Dzitko and J. Cretolle, "Observation and analysis of single event effects on-board the SOHO satellite", presented at RADECS2001, Grenoble, September 2001.

[38]   P. M. O'Niell, G. D. Badhwar and W. X. Culpepper, "Internuclear cascade - evaporation model for LET spectra of 200 MeV protons used for parts testing", IEEE Trans. Nucl. Sci., vol 45(6), pp. 2467-2474, Dec. 1998.

[39]   G. K. Lum, L. Robinette and A. Howard, "The use of proton testing for evaluating COTS: example of a commercial camera for ISS," IEEE Trans. Nucl. Sci., 48(6), pp. 1885-1892, Dec. 2001.

[40]   D. M. Hiemstra, S. Yu and M. Pop, "Single event upset characterisation of the Pentium MMX and Low Power Pentium MMX microprocessors using proton irradiation", Workshop Record, 2001 IEEE Radiation Effects Data Workshop, pp. 32-37, IEEE, 2001.

[41]   Final Report on "Radiation Effects in 2-D IR Sensors", ESTEC Contract 11755/95/NL/NB, Sira Electro-optics Ltd., September 1997.

[42]   C. A. Klein, "Bandgap dependence and related features of radiation ionization energies in semiconductors", J. Appl. Phys., vol. 39(4), pp. 2020-2038, 1968.

[43]   G. G. Pavlov and J. A. Nousek, "Charge diffusion in CCD X-ray detectors", Nucl. Instrum. Meth. A, vol. 428, pp. 348-366, 1999.

[44]   M. A. Xapsos, E. A. Burke, P. Shapiro and G. P. Summers, "Energy Deposition and Ionization Fluctuations Induced by Ions in Small Sites-An Analytical Approach", Radiation Research, vol. 137, pp. 152-161, 1994.

[45]   A. Claret, H. Dzitco and J. J. Engelmann, "Transient Particle Effects on the ISOCAM instrument on-board the infrared space observatory", IEEE-TNS vol., 46(6) pp. 1511-1518, 1999.

[46]   T. S. Lomheim, R. M. Shima, J. R. Angione, W. F. Woodward, D. J. Asman, R. A. Keller and L. W. Schumann, "Imaging Charge-Coupled Device (CCD) Transient Response to 17 and 50 MeV Proton and Heavy-Ion Irradiation", IEEE Trans. Nucl. Sci., vol. 37(6), pp. 1876-1885, 1990.

[47]   T. E. Dutton, W. F. Woodward and T. S. Lomheim, "Simulation of proton-induced transients on visible and infrared focal plane arrays in a space environment", Proc SPIE, vol. 3063, pp. 77-101, 1997.

[48]   A. Chugg and G. R. Hopkinson, "A new approach to modelling radiation noise in CCD's" IEEE Trans. on Nucl. Sci., vol. 45(3), pp. 1518-1523, 1998.

[49]   C. C. Liebe, "Charged-particle-induced noise in camera systems", IEEE Trans. on Nucl. Sci., vol. 48(4), pp. 1541-1549, 2001.

[50]   G. Reitz, R. Facius and H. Sandler, "Radiation protection in space", Acta Astronautica, vol. 35(4/5), pp. 313-338, 1995.

[51]   "Radiation Hazards to Crews of Interplanetary Missions: Biological Issues and Research Strategies", National Academy Press, 1996, available at http://www.national-academies.org/ssb/besrmenu.html

[52]   R. B. Setlow, "The U.S. National Research Council's views of the radiation hazards in space", Mutation research, vol. 430, pp. 169-175, 1999.

[53]   "Radiation and the International Space Station: Recommendations to Reduce Risk", National Academy Press, 2000, available at http://www.nas.edu/ssb/radissmenu.htm

[54]   Proc. NASA conference on "Shielding Strategies for Human Space Exploration", conference publication CP-3360, NASA, Dec. 1997.

[55]   T. C.-h. Yang, "Proton radiobiology and uncertainties", Radiation Measurements, vol. 30, pp. 383-392, 1999.

[56]   S. Iwai, T. Uehara, O. Sato, N. Yoshizawa, S. Furihata, S. Takagi, S.-i. Tanaka and Y. Sakamoto, "Overview of flunce to dose equivalent conversion coefficients for high energy radiations - calculational methods and results of effective dose equivalent and effective dose per unit particle

fluence", Proc. Conf. On Shielding Aspects of Accelerators, Targets and Irradiation Facilities (SATIF-3) , OECD Nuclear Energy Agency, 1998.

[57]   ICRP Publication 26, "Recommendations of the International Commission on Radiological Protection", Annals of the ICRP1, vol. 3, 1977, reprinted (with additions in 1987), superseded by ICRP publication 60.

[58]   ICRP Publication 60, "Recommendations of the International Commission on Radiological Protection", Annals of the ICRP, vol. 21 (1-3), Pergamon Press, Oxford, 1991.

[59]   Council Directive 96/29/EURATOM of 13 May 1996, Official Journal of the European Communities L159, vol. 39, 29 June 1996.

[60]   ICRU Report 51, "Quantities and units in radiation protection dosimetry", International Commission on Radiation Units and Measurements (ICRU, Bethesda, MA), 1993.

[61]   R. Kramer, M. Zankl, G. Williams and G. Drexler, "The calculation of dose from external photon exposures using reference phantoms and Monte Carlo methods. Part I: The male (Adam) and female (Eva) adult mathematical phantoms", Neuherberg: Gesellschaft fur Strahlen- und Umweltforschung, GSF-Bericht S-885, 1982

[62]   ICRU Report 33, "Radiation quantities and units", ", International Commission on Radiation Units and Measurements, (ICRU, Bethesda, MA), 1980.

[63]   D. T. Bartlett, "Radiation protection concepts and quantities for occupational exposure to cosmic radiation", Radiation protection Dosimetry, vol. 86(4), pp. 263-269, 1999.

[64]   J. W. Wilson, "Overview of radiation environments and human exposures", 34th Annual Meeting of the National Council on Radiation Protection, Washington DC, April 1998.

[65]   M. E. Velazquez, "Neurobiological problems in long-term deep space flights", Adv. Space Res., vol 22, pp. 171-183, 1998.

[66]   S. B. Curtis, M. E. Velazquez, J. W. Wilson, W. Atwell, M. Kim and J. Capala, "Cosmic ray hit frequencies in critical sites in the central nervous system", Adv. Space res., vol 22, pp. 197-207, 1998

[67]   T. C. Yang, K. A. George, H. Wu, D. Miller and J. Miller, "Cytogenetic effects of energetic ions with shielding", Adv. Space Res., vol. 22(12), pp. 1683-1690, 1998.

[68]   S. B. Curtis and J. R. Letaw, "Galactic cosmic rays and cell-hit frequencies outside the magnetoshere", Adv. Space Res., vol. 9(10), pp. 293-298, 1989.

[69]   J. W. Wilson, M. Kim, W. Schimmerling, F. F. Badavi, S. A. Thibeault, F. A. Cocinotta, J. L. Shinn and R. Kiefer, "Issues in space radiation protection: galactic cosmic rays", Health Physics, vol. 68(1), pp. 49-58, 1995.

[70]   S. B. Curtis, J. E. Nealy and J. W. Wilson, "Risk cross sections and their application to risk estimation in the galactic cosmic ray environment", Radiation Research, vol. 141, pp. 57-65, 1995.

[71]   F. A. Cucinotta, "Issues in risk assessment from solar particle events", Radiation Measurements, vol. 30, pp. 261-268, 1999.

[72]   C. S. Dyer, P. R. Truscott, C. L. Peerless, C. J. Watson, H. E. Evans, P. Knight, M. Cosby, C. Underwood, T. Cousins, R. Noulty and C. Maag, "Implications for space radiation environment models from CREAM & CREDO measurements over half a solar cycle", Radiation Measurements, vol. 30, pp. 569-578, 1999.

[73]   T. W. Armstrong and B. L. Colborn, "Predictions of secondary neutrons and their importance to radiation effects inside the international space station", Radiation Measurements, vol. 33, pp. 229-234, 2001.

[74]   R. H. Maurer, D. R. Roth, J. D. Kinnison, T. M. Jordan, L. H. Heilbronn, J. Miller and C. J. Zeitlin, "Neutron production from polyethylene and common spacecraft materials", IEEE Trans. Nucl. Sci., 48(6), pp. 2029-2033, Dec. 2001.

[75]   J. W. Wilson, F. F. Badavi, F. A. Cucinotta, J. L. Shinn, G. D. Badwhar, R. Silberberg, C. H. Tsao, L. W. Townsend and R. K. Tripathi, "HZETRN: description of a free-space ion and nucleon transport and shielding computer program" NASA TP-3495, 1995.

[76]   F. A. Cucinotta, J. W. Wilson, J. L. Shinn and R. K. Tripathi, "Assessment and requirements of nuclear reaction databases for GCR transport in the atmosphere and structures", Adv. Space Re., vol. 21(12), pp. 1753-1762, 1998.

[77]   J. W. Wilson, F. A. Cucinotta, H. Tai, S. Y. Chun. R. K. Tripathii and L. Sihver, "Transport of light ions in matter", Adv. Space Res., vol. 21(12), pp. 1753-1762, 1998.

[78]   J. L. Shinn, F. A. Cucinotta, J. W. Wilson, G. D. Badhwar, P. M. O'Niell and F. F. Badavi, "Effects of target fragmentation on evaluation of LET spectra from space radiation in low-earth orbit (LEO) environment: impact on SEU predictions", IEEE Transactions on Nuclear Science, vol. 42(6), pp. 2017-2025, Dec. 1995.

[79]   J. W. Wilson, F. A. Cucinotta, J. Miller, J. L. Shinn, S. Thibeault, R. C. Singleterry, L. C. Simonsen and M. H. Kimm, "Approach and issues relating to shield material dsign to protect astronauts from space radiation", Materials and Design, vol. 22, pp. 541-554, 2001.

[80]   F. A Cucinotta, R. Katz and J. W. Wilson, "Track structure model for radial distributions of electron spectra and event spectra from heavy ions", NASA TP-1998-208707, 1998.

[81]   G. D. Badwhar, J. Watts and T. E. Cleghorn, "Radiation dose from reentrant electrons", Radiation measurements, vol. 33, pp. 369-372, 2001.

[82]   B. A. Briskman, E. R. Klinshpont and V. I. Tupikov, "Space environment simulation at radiation test of nonmetallic materials", Nucl. Inst. Meth in Phys. Res. B, vol. 151, pp. 427-433, 1999.

[83]   "The Radiation Design Handbook", ESA PSS-01-609 issue 1, May 1993

[84]   "Nuclear and Space Radiation Effects on Materials", NASA SP-8053, June 1970

[85]   J R Laghari and A N Hammoud, "A brief survey of radiation effects on polymer dielectrics", IEEE Trans. Nucl. Sci., vol 37, pp. 1076-1083, 1990.

[86]   M. Tavlet and S. Ilie, "Behaviour of organic materials in radiation environment", Proc. RADECS99, pp. 210-215, 2000

[87]   F. L. Bouquet and J. W. Winslow, "Radiation effects response data for synthetic organic insulation and dielectrics", IEEE Trans. Nucl. Sci., vol 31(6), pp. 1387-1392, 1984.

[88]   T. Sasuga, S. Kawanishi, M. Nisshii, T. Seguchi and I. Kohno, "Effects of ion irradiation on the mechanical properties of several polymers", Radiation Physics and Chemistry, vol. 37(1), pp. 135-140, 1991.

[89]   A. R. Frederickson and S. Woolf, "Enhanced radiation shielding by space-charge fields in insulating slabs", J. Appl. Phys. Vol 81(2), pp. 834-839, 1997.

[90]   A. R. Frederickson, D. B. Cotts, J. A. Wall and F. l. Bouquet, "Dielectric material in the space environment", SAMPE Journal, pp. 12-16, March/April 1985.

[91]   F. L. Bouquet "Radiation thresholds for synthetic elastomers", IEEE Trans. Nucl. Sci., vol 32(6), pp. 4254-4259, 1985.

[92]   H. Bamsemir and O. Haider, "Fibre composite structures for space applications - recent and future developments", Cryogenics, vol. 38, pp. 51-59, 1998.

[93]   S. M. Spiessberger, K. Humer, E. K. Tshegg, H. W. Weber and H. Gerstenberg, "Reactor irradiation effects on the ultimate tensile and the interlaminar shear strength of carbon fibre reinforced epoxies at 77K", Cryogenics, vol. 38, pp. 79-83, 1998.

[94]   G. F. Sykes and D. E. Bowles, "Space radiation effects on the dimensional stability of a toughened epoxy graphite composite", SAMPE Quarterly, pp. 39-45, July 1986.

[95]   S. Egusa, "Mechanism of radiation-induced degradation in mechanical properties of polymer matrix composites", J. Materials Science, vol. 23, pp. 2753-2760, 1988.

[96]   S. G. Burnay, "Effect of pre-stressing on the behaviour of CFRP under gamma irradiation", ESA Journal, vol. 16, pp. 435-445, 1992.

[97]   J. M. Pintando and J. Miguel, "Effects of γ-radiation on mechanical behaviour of carbon/epoxy composite materials", Cryogenics, vol. 38, pp. 85-89, 1998.

[98]   E. W. Taylor, J. Grote, J. Zetts, J. E. Winter, A. D. Sanchez and D. Craig," In situ high energy proton irradiation of nonlinear organic modulator materials for space environments", Proc. SPIE, vol. 4134, pp. 25-30, 2000.

[99]   D. A. Russell, L. B. Fogdall and G. Bohnhoff-Hlavacek, "Simulated space environment testing on thin films", NASA CR-2000-210101, April 2000.

[100]   R. L. Alstatt and D. L. Edwards, "Modeling of natural space ionising radiation effects on external materials", Proc. SPIE, vol. 4134, pp. 231-242, 2000.

[101] C. Barnes and R. Greenwell, "Radiation effects in photonic modulator structures", Proc SPIE, vol. 2482, pp. 48-98, 1995.

[102] C. Barnes, G. Swift, A. Johnston, B. Rax and K. LaBel, "Radiation effects considerations for the application of photonics in space systems", IEEE 1998 Aerospace Conference, vol. 2, pp. 219-239, 1998.

[103] F. Brioschi, A. Caridi, E. Cereda, G. M. Braga, Marcazzan and E. Zanzoterra, "Radiation effects on laser crystals for space applications", Nucl. Instrum. Meth. B, vol. 66, pp. 357-360, 1992.

[104] U. Roths, M. Troebs, T. Graf, J. E. Balmer and H. P. Weber, "proton and gamma radiation tests on nonlinear crystals", Applied Optics, Vol 41(3), pp. 464-469, 2002.

[105] D. L. Griscom, M. E. Gingerich and E. J. Friebele, "Radiation-induced defects in glasses: origin of power-law dependence of concentration on dose", Phys. Rev. Lett., vol. 71(7), pp. 1019-1022, 1993.

[106] D. T. H. Liu and A. R. Johnston, "Theory of radiation-induced absorption in optical fibers", Optics Letters, vol. 19(8), pp. 548-550, 1994.

[107] M. Van Uffelen, Ph. Jucker and Ph. Fenaux, "Radiation resistance of fiberoptic components and predictive models for optical fiber systems in nuclear environments", Proc. RADECS97, pp. 445-452, IEEE, 1998.

[108] R. H. West, "Predicting the radiation induced loss in Ge doped optical fibres at different temperatures", Proc. RADECS99, pp. 483-490, IEEE, 2000.

[109] E. W. Taylor, S. J. McKinney, A. D. Sanchez, A. H. Paxton, D. M. Craig, J. E. Winter, R. Ewart, K. Miller, T. O'Connor and R. Kaliski, "Gamma-ray induced effects in Erbium-doped fiber optic amplifiers". Proc. SPIE, vol. 3440, pp. 16-23, 1998.

[110] X. Glavas, L. Lembo, W. Haraki, S. Claxton and R. Greenwell, "Radiation test results of polarization maintaining fiber at 1.55 µm over a wide temperature range", Proc. SPIE, vol. 3440, pp. 120-130, 1998.

[111] M. Fruit, A. Gusarov, D. Doyle and G. Ulbrich, "Radiation impact on space borne optics the 'dose coefficients' approach", Proc. SPIE, vol. 3872, pp. 60-71, 1999.

[112] A. J. Marker, J. S. Hayden and B. Speit, "Radiation resistant optical glasses", Proc. SPIE, vol. 1485, pp. 160-172, 1991.

[113] M. Fruit, A. Gusarov, D. Doyle, G. Ulbrich and A. Hermanne, "Space radiation sensitivity of glasses: first results towards a comprehensive dose coefficients database", Proc. SPIE, vol. 4134, pp. 261-267, 2000.

[114] Private Communication, Dominic Doyle (ESTEC), 2001.

[115] D. L. Edwards, K. Herren, M. Hayden, K. McDonald, J. A. Sims and C. L. Semmel, "Investigation into radiation induced compaction of Zerodur", NASA Tech. Mem, 108505, March 1996.

[116] P. L. Higby, E. J. Freibele, C. M. Shaw, M. Rajaram, E. K. Graham, D. L. Kinser and E. G. Wolff, "Radiation effects on the physical properties of low-expansion glasses and ceramics", J. Am. Ceram. Soc., vol. 71(9), pp. 796-802, 1988.

[117] C. I. Merzbacker, E. J. Freibele, J. A. Ruller and P. Matic, "Finite element analysis of deformation in large optics due to space environment radiation", Proc. SPIE, vol. 1533, pp. 222-228, 1991.

[118] P. L. P. L. Higby, C. G. Askins, J. A. Ruller and E. J. Freibele, " Radiation effects on the low temperature coefficient of thermal expansion of low-CTE materials", Proc SPIE, vol. 970, pp. 70-77, 1988.

[119] R. Koga, S. D. Pinkerton, S. C. Moss, D. C. Meyer, S. LaLumondiere, S. J. Hansel, K. B. Crawford and W. R. Crain, "Observation of Single Event Upsets in Analog Microcircuits", IEEE Trans. Nucl. Sci., vol. 40, pp. 1838-1844, 1993.

[120] R. Ecoffet, R. S. Duzellier, P. Tastet, C. Aicardi, and M. Labrunee, "Observation of Heavy Ion Induced Transients in Linear Circuits", 1994 IEEE Radiation Effects Data Workshop Record, pp. 72-77, 1994.

[121] D. K. Nichols, J. R. Coss, T. F. Miyahira and H. R. Schwartz, "Heavy Ion and Proton Induced Single Event Transients in Comparators, IEEE Trans. Nucl. Sci., vol. 43, pp. 2960-2967, 1996.

[122] S. H. Penzin, W. R. Crain, K. B. Crawford, S. J. Hansel, J. F. Kirshman and R. Koga, "Single Event Effects in Pulse Width Modulation Controllers", IEEE Trans. Nucl. Sci., vol. 43, pp. 2968-2973,1996.

[123] R. Koga, S. H. Penzin, K. B. Crawford, W. R. Crain, S. C. Moss, S. D. Pinkerton, S. D. LaLumondiere and M. C. Maher," Single Event Upset (SEU) Sensitivity Dependence of Linear Integrated Circuits (ICs) on Bias Conditions", IEEE Trans. Nucl. Sci., vol. 44, pp. 2325-2332, 1997

[124] R. Harboe-Sorensen, F. X. Guerre, H. Constans, J. van Dooren, G. Berger and W Hajdas, "Single Event Transient SEU Characterisation of Analog ICs for ESA's Satellite, Proc. RADECS 99, 573-581, IEEE, 2000.

[125] R. Koga, S. H. Crain, K. B. Crawford, S. C. Moss, S. D. LaLumondiere and J. W. Howard, Jr., "Single Event Transient (SET) Sensitivity of Radiation Hardened and COTS Voltage Comparators", 2000 IEEE Radiation Effects Data Workshop Record, 53-60, 2000.

[126] P. Adell, R. D. Schrimpf, H. J. Barnaby, R. Marec, C. Charty, P.Calvel, C. Barillot and O. Mion, "Analysis of Single-Event Transients in Analog Circuits", IEEE Trans. Nucl. Sci., vol. 47, pp. 2616-2623, 2000.

[127] A. H. Johnston, G. M. Swift, T. F. Miyahira and L. D. Edmonds, "A Model for Single-Event Transients in Comparators", IEEE Trans. Nucl. Sci., vol. 47, pp. 2624-2633, 2000.

[128] T. L. Turflinger, "Single Event Effects in Analog and Mixed-signal Integrated Circuits, IEEE Trans. Nucl. Sci., 43, pp. 594-603, 1996.

[129] S. Bee, G. R. Hopkinson, R. Harboe-Sørensen, L. Adams and A. Smith, "Heavy-ion study of single event effects in 12- and 16-Bit ADCs", Workshop Record 1998 IEEE Radiation Effects Data Workshop, pp. 58-67, 1998.

[130] S. Bee, G. R. Hopkinson, R. Harboe-Sorensen L. Adams and A. Smith, "252 Cf measurements of single event effects in ADCs", Workshop Record 1997 RADECS Data Workshop, pp. 81-88, 1997.

[131] R. L. Pease, A. Sternberg, L. Massengill, R. Schrimpf, S. Buchner, M. Savage, J. Titus and T. Turflinger, "Critical charge for single event transients in bipolar linear circuits", IEEE Trans. Nucl. Sci., 48(6), pp. 1966-1972, Dec. 2001.

[132] C. Poivey, J. W. Howard, S. Buchner, K. A. LaBel, J. D. Forney, H. S. Kim and A. Assad, "Development of a test methodology for single-event transients (SETs) in linear devices", IEEE Trans. Nucl. Sci., 48(6), pp. 2180-2186, Dec. 2001.

[133] M. W. Savage, "T. Turflinger, J. W. Howard and S. Buchner, "A compendium of single event transient data", Workshop Record, 2001 IEEE Radiation Effects Data Workshop, pp. 134-141, IEEE, 2001.

[134] M. Alexander and D. F. Bowers, "SPICE-compatible Op Amp macro-modules ", Electronics design News, Feb/March 1990, pp. 13-155 to 13-170. Also available as Analog Devices application Note AN-138.

[135] www.beigebag.com

[136] R. Marec, C. Chatry, P. Adell, O. Mion, C. Barillot and P. Calvel, "Single event transient hardness assurance methodology", Presented at RADECS 2001, Grenoble, September 2001.

[137] P.W. Marshall, C. Poivey, C. J. Marshall, R. A. Reed and K. A. LaBel, "Test needs and error rate prediction approaches for single event transients in fiber optic link detectors and optocouplers", Presented at RADECS 2001, Grenoble, September 2001.

[138] P.W. Marshall, C. J. Dale, M. A. Carts and K. A. LaBel, "Particle-induced bit errors in high performance fiber optic data links for satellite data management," IEEE Trans. Nucl. Sci., Vol. 41, pp. 1958-1965, Dec. 1994.

[139] A.H. Johnston, T. Miyahira, G. M. Swift, S. M. Guertin and L. D. Edmonds, "Angular and energy dependence of proton upset in optocouplers," IEEE Trans. Nucl. Sci., Vol. 47, No. 6, pp. 1335-1341, Dec. 1999.

[140] T. P. Ma and P. V. Dressendorfer, "Ionizing Radiation Effects in MOS Devices and Circuits", John Wiley & Sons, New York, 1989.

[141] J. R. Solin, "Electron collision dose enhancement", IEEE Trans. Nucl. Sci., vol. 47(6), pp. 2447-2450, Dec. 2000.

[142] J. R. Solin, "The GEO total ionising dose", IEEE Trans. Nucl. Sci., vol. 45(6), pp. 2964-2971, Dec. 1998.

[143] G. J. Brucker, S. Kronenburg and F. Genter, "Effects of package geometry, materials and die design on energy dependence of pMOS dosimeters", IEEE Trans. Nucl. Sci., vol. 42(1), pp. 33-40, Feb. 1995.

[144] T. R. Oldham, K. W. Bennett, J. Beaucour, T. Carriere, C. Poivey and P. Garnier, "Total dose failures in advanced electronics from single ions", IEEE Trans. on Nucl. Sci., vol. 40(6), pp. 1820-1830, Dec. 1993.

[145] L. D. Edmonds, S. M. Guertin, L. Z. Scheick, D. Nguyen, and G. M. Swift, " Ion-Induced stuck bits in 1T/1C SDRAM cells", IEEE Trans. Nucl. Sci., 48(6), pp. 1925-1930, Dec. 2001.

[146] C. Dufour, P. Garnier, T. Carriere, J. Beaucour, R. Ecoffet, and M. Labrunee, "Heavy ion induced single hard errors on submicronic memories," IEEE Trans. Nucl. Sci., vol. 39(6) pp. 1693-1697, Dec. 1992.

[147] J. C. Pickel, "Single event damage effects in cryogenic CMOS microelectronics", IEEE Trans. Nucl. Sci., vol. 43(3), pp. 912-917, Dec. 1996.

[148] C. S. Dyer, P. R. Truscott, H. E. Evans, N. Hammond, C. Comber, S. Battersby, "Calculations and observations of induced radioactivity in spaceborne materials," IEEE Trans. Nucl. Sci., vol. 41(3), pp. 438-444, June 1994.

[149] M. Bavdaz, A. Peacock and A. Owens, "Future space applications of compound semiconductor X-ray detectors", Nucl. Instrum. Meth. A, Vol. 458, pp. 123-131, 2001.

[150] E. L. Hull, R. H. Pehl and L. S. Varnell, "The effects of 199 MeV proton radiation damage on CdZnTe photon detectors", IEEE Trans. Nucl. Sci., vol. 44(3) 870-873, June 1997.